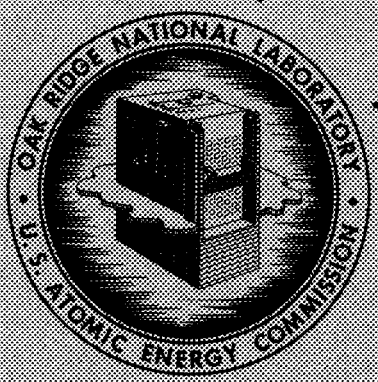


ORNL
MASTER COPY

ORNL-3438 *Def*
UC-25 - Metals, Ceramics, and Materials
TID-4500 (20th ed.)

INVESTIGATION OF THE WETTABILITY OF VARIOUS
PURE METALS AND ALLOYS ON BERYLLIUM

Ralph Gerald Gilliland



OAK RIDGE NATIONAL LABORATORY
operated by
UNION CARBIDE CORPORATION
for the
U.S. ATOMIC ENERGY COMMISSION

LEGAL NOTICE

This report was prepared as an account of Government sponsored work. Neither the United States, nor the Commission, nor any person acting on behalf of the Commission:

A. Makes any warranty or representation, expressed or implied, with respect to the accuracy, completeness, or usefulness of the information contained in this report, or that the use of any information, apparatus, method, or process disclosed in this report may not infringe privately owned rights; or

B. Assumes any liabilities with respect to the use of, or for damages resulting from the use of any information, apparatus, method, or process disclosed in this report.

As used in the above, "person acting on behalf of the Commission" includes any employee or contractor of the Commission, or employee of such contractor, to the extent that such employee or contractor of the Commission, or employee of such contractor prepares, disseminates, or provides access to, any information pursuant to his employment or contract with the Commission, or his employment with such contractor.

ORNL-3438

Contract No. W-7405-eng-26

Metals and Ceramics Division

INVESTIGATION OF THE WETTABILITY OF VARIOUS
PURE METALS AND ALLOYS ON BERYLLIUM

Ralph Gerald Gilliland

Submitted as a thesis to the Graduate Council of the University
of Tennessee in partial fulfillment of the requirements for the
degree of Master of Science

DATE ISSUED

MAY 29 1963

OAK RIDGE NATIONAL LABORATORY
Oak Ridge, Tennessee
operated by
UNION CARBIDE CORPORATION
for the
U. S. ATOMIC ENERGY COMMISSION

ACKNOWLEDGMENT

The author wishes to thank Dr. E. E. Stansbury for his generous advice and encouragement throughout the course of this investigation and for his contributions to the preparation of this manuscript.

The author was very fortunate in having been able to perform his experimental work at the Oak Ridge National Laboratory. It would be impossible to acknowledge the contributions of the large number of Laboratory personnel whose comments, advice, and direct assistance were invaluable in the accomplishment of this work. Special gratitude, however, is extended to G. M. Slaughter for his help and advice in all phases of the investigation.

The assistance of J. D. Hudson of the Welding and Brazing Group and R. V. Tindula, Co-op student from Virginia Polytechnic Institute, Metals and Ceramics Division during the preliminary testing period of this investigation is gratefully acknowledged.

Metallographic work was performed by S. E. Spencer and E. R. Boyd, and the macrophotographs were prepared by J. C. Gower and E. P. Griggs, all of the Metallography Group.

The fine drawings presented here were the work of Mrs. Gail Gilliland, wife of the author.

The author also wishes to express his appreciation to Mrs. Geneva Harris, Miss Susan Thompson, and Mrs. Frances Scarboro of the Metals and Ceramics Division Reports Office for their prompt preparation of this manuscript.

Thanks are also extended to the Union Carbide Nuclear Company for its employee educational assistance program, and to the Gas-Cooled Reactor Program for providing financial support for this work.

TABLE OF CONTENTS

CHAPTER	PAGE
I. SUMMARY	1
II. INTRODUCTION	3
III. OBJECTIVES	9
IV. PRIOR WORK	10
V. EXPERIMENTAL PROCEDURE	12
VI. RESULTS AND DISCUSSION	30
Qualitative Discussion of Contact Angle	
Measurements	30
Results of Metallographic Analysis	33
Silver-Beryllium	34
Gold-Beryllium	37
Copper-Beryllium	40
Palladium-2.1 Weight Per Cent Beryllium-	
Beryllium	49
Germanium-Beryllium	54
Aluminum-Beryllium	54
Zirconium-5 Weight Per Cent Beryllium-Beryllium .	58
Titanium-6 Weight Per Cent Beryllium-Beryllium . .	58
Results of Surface Tension Calculation	62
VII. CONCLUSIONS AND RECOMMENDATIONS	68
Conclusions	68
Recommendations	69

	PAGE
APPENDIX	72
Equipment	72
Furnace and Vacuum Equipment	72
Photographic Equipment	75
Arc-Melting Equipment and Procedure	75
Metallographic Equipment and Procedure	75
Sample Calculations	78
The Sessile-Drop Method	78
Typical Calculation of γ_{LV}	82
Typical Calculation of γ_{SL} , W_{ad} , and S_{LS}	85
LIST OF REFERENCES	87
BIBLIOGRAPHY	90

CHAPTER I

SUMMARY

Beryllium has a combination of physical and mechanical properties which makes it attractive for wide use as a reflector, moderator, and fuel cladding material in the nuclear field and in gyroscopes and other flight components in the aircraft industry. In most of these applications, beryllium must be joined to itself or other metals and brazing is one of the most useful joining procedures. The determination of the wetting behavior of certain pure metals and alloys on beryllium is very important in the development of brazing alloys for joining beryllium.

The wetting behavior of liquid silver, gold, germanium, aluminum, copper, palladium-2.1 weight per cent beryllium, zirconium-5 weight per cent beryllium, and titanium-6 weight per cent beryllium on the surface of solid beryllium is discussed. In general, the wetting of these metals was investigated at 50 and 100°C above their melting points in argon and in vacuum. The general experimental method employed the use of sessile-drop techniques for the evaluation of wettability and the associated calculations.

Interfacial contact angles between drop and solid were measured for the various metals as a function of time, temperature, and atmosphere. The results of these measurements indicate that the wetting of beryllium follows the general theoretical pattern; that is, it increases with increasing temperature. Effects of vacuum and argon

environments showed no general trend, but instead, the behavior with regard to these environments appeared to be dependent upon the particular system being tested.

Extensive metallographic examination revealed that beryllium had alloyed, to varying extents, with gold, silver, copper, germanium, and palladium—2.1 weight per cent beryllium and that the liquid had penetrated into the solid. Little or no beryllium alloying was observed on samples wetted with aluminum, zirconium—5 weight per cent beryllium, and titanium—6 weight per cent beryllium, although wetting was observed for the latter two cases.

Surface tension calculations, using the sessile-drop technique, were made for the three systems which revealed little or no penetration into the beryllium. The calculations of the liquid-vapor and liquid-solid surface tensions, the work of adhesion, and the coefficient of spreading served as a qualitative means of measuring the wettability of beryllium by these three metals. The results indicated that the titanium—6 weight per cent beryllium alloy produced the lowest liquid-vapor and liquid-solid surface tensions and highest work of adhesion and spreading coefficients, indicating the best overall wetting characteristics.

CHAPTER II

INTRODUCTION

Beryllium, in the past, has been considered primarily as an alloying addition to other metals, principally copper. This usage still represents at least 80 per cent of the total amount manufactured. Currently, the pure metal has become attractive to the nuclear and aircraft industries because of its very low thermal-neutron-absorption cross section, its high thermal conductivity and specific heat, its high elastic modulus, and its high strength to weight ratio (1-4). The use of pure beryllium in these applications is made difficult by such undesirable properties as high toxicity and generally poor fabricability; however, one of the greatest problems has been that of joining and, in particular, brazing.

Beryllium, in general, is very difficult to braze successfully. Industrial experience has indicated that poor flow and brittle joints are commonly encountered (5,6). Also, very little information is available on the use of brazing for high-temperature service. In order to fruitfully develop brazing alloys for joining this material, information on the wetting behavior of different liquid metals is important. A comprehensive theory of the wetting or spreading of liquids on solid surfaces has been presented by Hawkins (7). The complete and detailed derivation of the quantitative relationships will not be repeated here; only the necessary definitions and equations relating to the discussion are presented.

The free surface energy of a substance at constant temperature (T), pressure (p), and concentration (N) is defined as

$$\left(\frac{\partial F}{\partial A}\right)_{p,T,N} \equiv \gamma \equiv \text{free surface energy (usually dynes) per square centimeter,} \quad (1)$$

where

F = the free energy of the substance,

A = its surface (or interfacial) area.

The thermodynamic condition for spreading to occur is that, for an incremental increase in area, the entire system will have

$$dF < 0 . \quad (2)$$

Conversely, for nonspreading

$$dF > 0 . \quad (3)$$

If it is assumed that in the course of spreading of a liquid, L, in equilibrium with its own vapor, V, on a surface, S, in equilibrium with its own vapor, the following area relation exists:

$$dA_{LV} = dA_{SL} = -dA_{SV} , \quad (4)$$

then

$$\left(\frac{\partial F}{\partial A}\right)_{p,T} = \gamma_{LV} + \gamma_{SL} - \gamma_{SV} . \quad (5)$$

where

γ_{IV} = the liquid-vapor surface energy,

γ_{SL} = the solid-liquid surface energy,

γ_{SV} = the solid-vapor surface energy.

Let $-dF/dA$ be designated as the final spreading coefficient, S_{IS} ; then, at constant temperature and pressure,

$$S_{IS} = \gamma_{SV} - (\gamma_{IV} + \gamma_{SL}) . \quad (6)$$

As a measure of the attraction between different materials, the work of adhesion can be obtained as

$$W_{ad} = (\gamma_{IV} + \gamma_{SV}) - \gamma_{IS} . \quad (7)$$

The work of adhesion represents the decrease in energy in bringing together a unit area of liquid surface and a unit area of solid surface to form a unit area of interface.

Experimentally, it is observed that liquids placed on solid surfaces usually will not completely wet but rather remain as a drop having a definite contact angle between the liquid and solid phases. This condition is illustrated in Figure 1. The Young and Dupré equation (8) permits the determination of change in surface free energy, ΔF^S , accompanying a small change in solid surface covered, ΔA . Thus,

$$\Delta F^S = \Delta A (\gamma_{SL} - \gamma_{SV}) + \Delta A \gamma_{IV} \cos (\theta - \Delta\theta) . \quad (8)$$

Unclassified
Y-49251

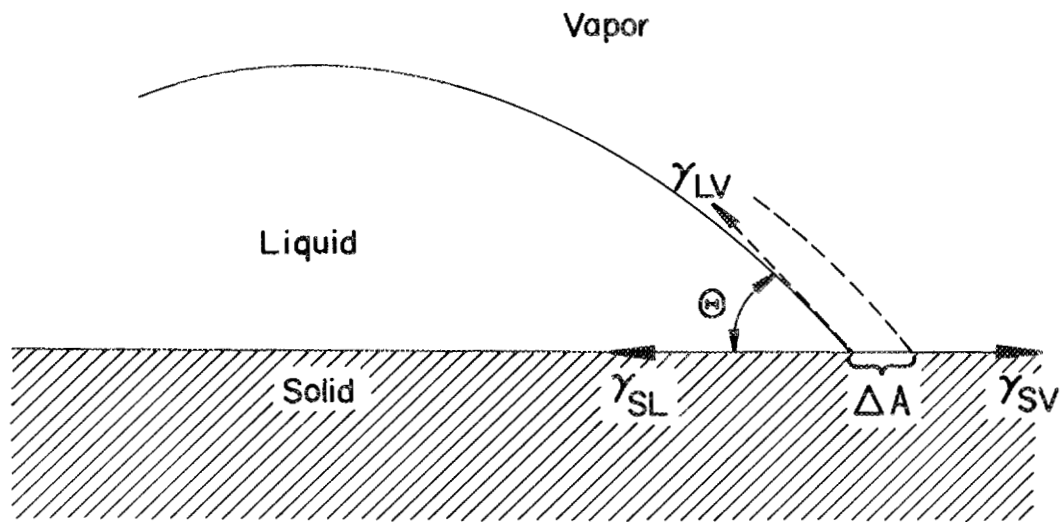


Figure 1. A sessile drop showing the vectors of the surface energies for the system.

At equilibrium,

$$\lim_{\Delta A \rightarrow 0} \frac{\Delta F^S}{\Delta A} = 0$$

and

$$\gamma_{SL} - \gamma_{SV} + \gamma_{LV} \cos \theta = 0 \quad (9)$$

or

$$\gamma_{SL} = \gamma_{SV} - \gamma_{LV} \cos \theta . \quad (10)$$

With this relationship combined with equation 7, we obtain

$$W_{ad} = \gamma_{LV} (1 + \cos \theta) . \quad (11)$$

In equations 9 and 10 it can be seen that θ will be greater than 90 degrees when γ_{SL} is larger than γ_{SV} and less than 90 degrees when the reverse is true. For greater wetting, θ should be as small as possible so that $\cos \theta$ approaches unity.

The interfacial tension between a solid and a liquid may be considered as a measure of the fit or misfit between the two phases. Qualitatively, the smaller the difference in misfit that is present the smaller will be the magnitude of the surface tension. The lower limit of any interfacial tension may be considered as that tension existing between the solid and liquid phases of the same metals. In cases where considerable interaction occurs between the solid and liquid phases, the measurement of any surface tension becomes

meaningless. This situation exists as a result of the continuous concentration changes occurring in both phases produced by the rapid atom movement of material across the interface. In situations such as these, the mutual solubility of the phases in each other and the possibility of intermediate phase formation at the interface must be considered.

CHAPTER III

OBJECTIVES

The general objective of this investigation was to determine the wetting behavior of pure gold, silver, germanium, aluminum, copper, and the binary alloys of titanium-6 weight per cent beryllium, zirconium-5 weight per cent beryllium, and palladium-2.1 weight per cent beryllium on solid beryllium. These metals are likely candidates as components of brazing alloys for elevated-temperature service.

The specific objectives were (1) to measure the contact angles of the molten metals on beryllium as a function of test temperature, time at temperature, and atmosphere; (2) to investigate the solid-liquid interfacial reactions occurring as a function of test temperature and atmosphere; and (3) to calculate the liquid-vapor and interfacial surface tensions for those systems where interfacial reactions did not appear to occur or were small.

CHAPTER IV

PRIOR WORK

Some effort has been made in an attempt to develop solders and brazing alloys for joining beryllium to itself and to other materials; this work has been concentrated on applications having service temperatures less than 538°C. Very little published work has appeared in the literature concerning the basic wetting behavior of molten metals on beryllium.

Cohen (9) conducted preliminary work on the wetting of beryllium using beryllium-rich binary alloys of silicon and silver. He found that the addition of 20 atomic per cent silver to beryllium reduced the interfacial reaction which existed when pure liquid silver was in contact with beryllium, but the wetting of the alloy on beryllium was nil. It was also found that the beryllium-silicon alloys did not wet the base material.

Monroe et al. (10) studied the wetting of beryllium with aluminum and its alloys. They found that, although the joints were often porous, joints of reasonably good quality could be made with an aluminum-12 weight per cent silicon alloy.

Zunick and Illingworth (11) and Wikle and Magalski (12) have successfully brazed beryllium to other metals (mainly refractory metals) using pure silver and the silver-copper eutectic in vacuum.

The author has performed preliminary work on the development of beryllium brazing alloys for high-temperature, helium-atmosphere applications (13). A ternary alloy composed of 49 weight per cent titanium-49 weight per cent copper-2 weight per cent beryllium was found to join small sections of beryllium and stainless steel. The leak-tight dissimilar joints withstood high-temperature thermal cycles while under irradiation.

The sessile-drop method, used in this study for the calculation of the liquid-vapor surface energies, is presented by Ellefson and Taylor (14). These investigators used this technique to study the surface properties of fused salts and glasses.

CHAPTER V

EXPERIMENTAL PROCEDURE

Several 3/8-inch-diameter \times 12-inch-long beryllium rods were procured from the Brush Beryllium Company, Cleveland, Ohio. This material was manufactured using hot-pressing techniques followed by machining to final size. The randomly oriented grain structure of the beryllium metal produced by this fabrication procedure is represented by the photomicrograph of Figure 2.

A suitable brazing alloy is one having a melting point lower than the melting point of the base metal and which exhibits a minimum tendency to dissolve the base metal; it is of course essential that wetting occurs. The materials used in this investigation were selected with these points in mind and they are presented, together with their melting points, in Table I. Prior work by other investigators has indicated that aluminum-, copper-, and silver-base alloys appear promising for brazing beryllium (10,15). Gold, copper, and germanium possess melting points in the temperature range of interest and were consequently considered to merit investigation. Previous work by the writer has demonstrated that titanium, zirconium, and palladium are promising as major constituents of alloys for brazing beryllium (16-18). In the present research, these elements have been prealloyed with beryllium in order to obtain allowable melting points; the selection of beryllium being made in order to keep the number of variables to a

Unclassified
Y-84065

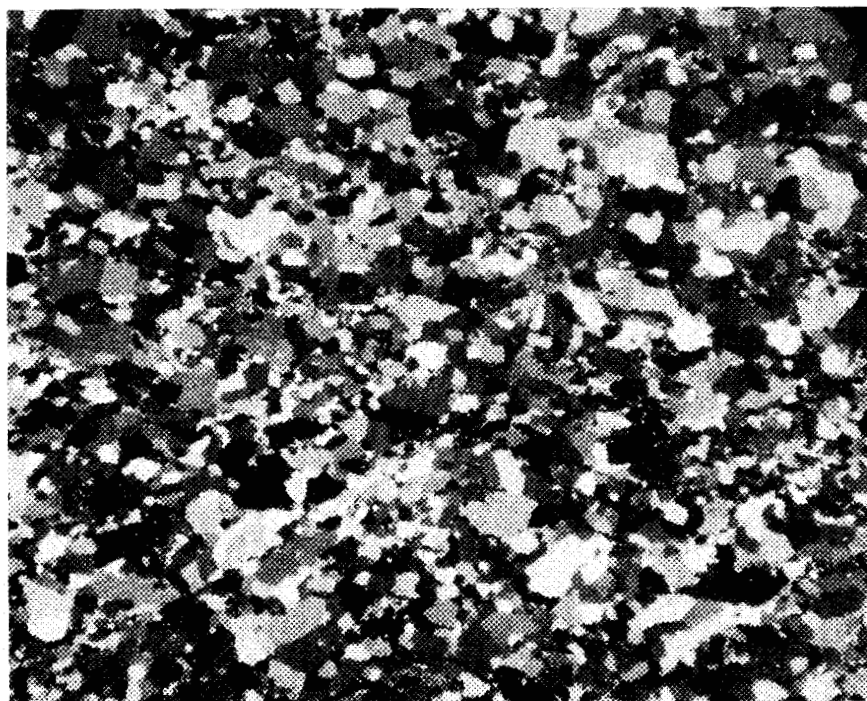


Figure 2. Photomicrograph of the beryllium metal showing the randomly oriented grain structure. Polarized light. 100X.

TABLE I
MATERIALS AND TEST TEMPERATURES USED IN
THE BERYLLIUM WETTABILITY STUDY

Material.	Melting Point (°C)	Test Temperature (°C)
Gold	1063	1070
Copper	1083	1108, 1133
Aluminum	660	710, 760
Silver	960	1010, 1060
Germanium	950	1000, 1050
Ti-6 wt % Be	1025	1075, 1125
Zr-5 wt % Be	980	1030, 1080
Pd-2.1 wt % Be	930	980, 1030

minimum. The solubility of beryllium in liquid aluminum and the liquid binary alloys is quite low, but its solubility in liquid silver, gold, and copper was somewhat higher at the temperatures under investigation. The solubility of beryllium in liquid germanium is not known.

The wetting studies were performed using metals of very high purity which had been arc melted into buttons as described in the Appendix. Both the beryllium and the metals to be melted on it were analyzed spectrographically. The results are presented in Table II.

The wettability study consisted of testing in both argon and vacuum atmospheres at the temperatures indicated in Table I, page 14. In most cases the testing temperatures were 50 and 100°C above the melting points of the materials studied. The test temperatures for the gold and copper experiments were lowered, however, to reduce the extent of interfacial reaction and beryllium alloying observed during preliminary testing.

Wettability data were obtained using the sessile-drop method, as described by Quincke (19) and Adam (20). This procedure is advantageous for (1) it is a static method that is suitable for high-temperature testing, and (2) it allows the measurement of contact angles coincidentally with the determination of the liquid-vapor surface energies.

The sample preparation for the wettability tests consisted initially of machining the 3/8-inch-diameter beryllium rods into wafers or pads of 1/8-inch thickness. The arc-melted metal buttons were either

TABLE II
 CHEMICAL ANALYSES OF BERYLLIUM-BASE METAL AND THE METALS TO BE MELTED ON IT

Material	Impurities Analyzed for												
	BeO (wt %)	Be (%)	Fe	Al	Mg	Si	C (ppm)	Ca	Mn	Pb	Cu	N	O
Beryllium	1.37	Bal	1300	550	50	300	1200	100	100	--	--	420	4400
Silver	--	--	172	60	--	--	--	--	--	--	323	120	2200
Gold	--	--	--	--	--	--	--	--	--	10	--	--	21
Aluminum	--	--	--	Bal	--	--	--	--	--	--	--	--	57
Copper	--	--	--	--	--	--	--	--	--	--	Bal	--	45
Germanium	--	--	--	--	--	--	--	--	--	--	--	10	20
Ti-6 wt % Be	--	6.11	--	--	--	--	--	--	--	--	--	21	560
Pd-2.1 wt % Be	--	2.17	--	--	--	--	27	--	--	--	--	--	38
Zr-5 wt % Be	--	4.74	--	--	--	--	--	--	--	--	--	17	440

machined into 1/8-inch cubes or remelted into smaller buttons approximately 1/8- to 3/16-inch diameter.

The machined beryllium pad was precleaned by etching using an aqueous solution of 2 parts HF, 3 parts lactic acid, 5 parts HNO₃, and 10 parts H₂O. After this preparation, both the pad and the metal to be melted were assembled on a molybdenum furnace boat in the manner illustrated in Figure 3. The methods for obtaining vacuum and inert-gas atmosphere, together with a description of the furnace equipment, are presented in the Appendix. A discussion of the optical system used in the measurement of contact angles is also presented in the Appendix.

After carefully loading the test assembly into the vacuum muffle furnace and precisely leveling the beryllium pad to permit accurate optical measurements, the following procedure was used for each wettability test:

1. The ceramic muffle (at room temperature) was evacuated to less than 1×10^{-5} torr. Intermediate purging of the system using high-purity argon was incorporated to improve the purity of the gas remaining in the system.
2. The furnace, already at test temperature, was then rolled over the muffle and the system was allowed to come to test temperature.
3. After thermal equilibrium was established, individual photographs of the liquid metal-beryllium sample were taken at

Unclassified
Y-48031

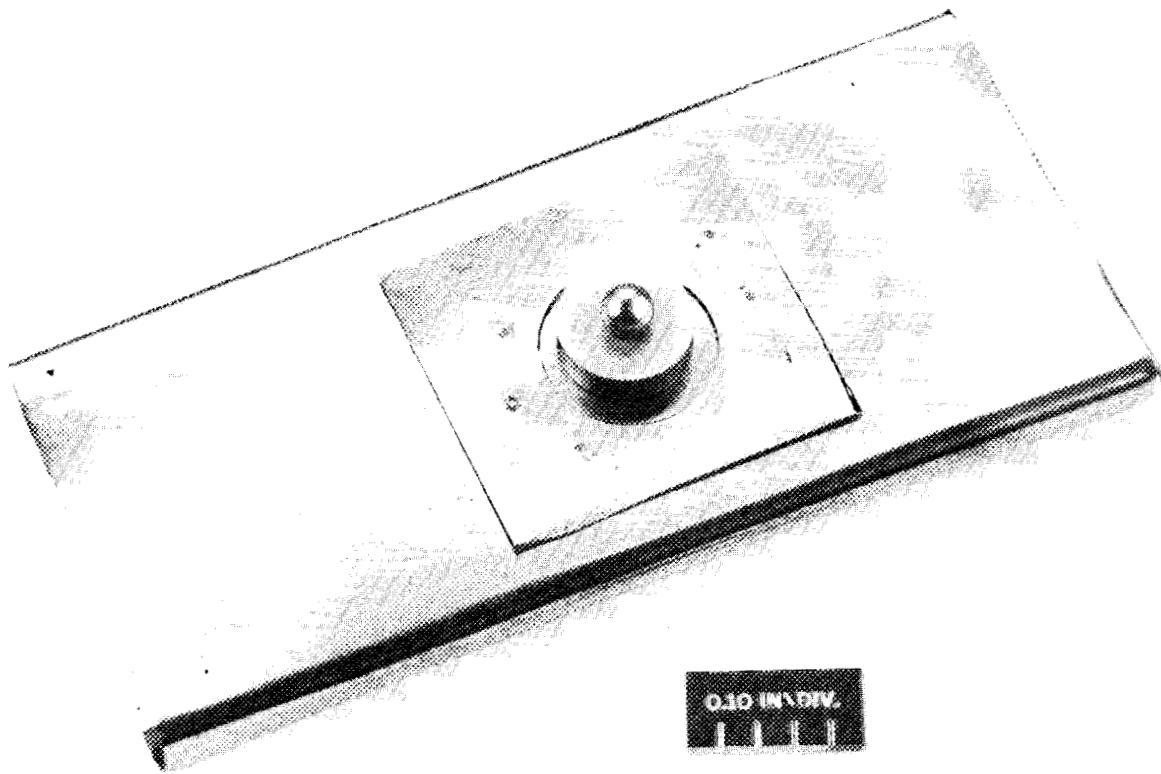


Figure 3. Beryllium pad, metal to be melted, and furnace boat ready for insertion in the furnace muffle. 7X.

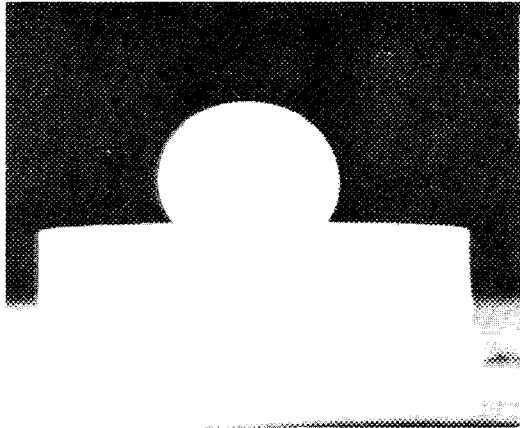
time intervals of 0, 15, 45, 90, and 150 seconds. Timing was begun at the moment temperature stabilization was attained as indicated by the muffle temperature recorder and controller.

4. The hot furnace was rolled away from the muffle immediately after the last picture was taken and the specimen was allowed to cool to approximately room temperature inside the muffle.

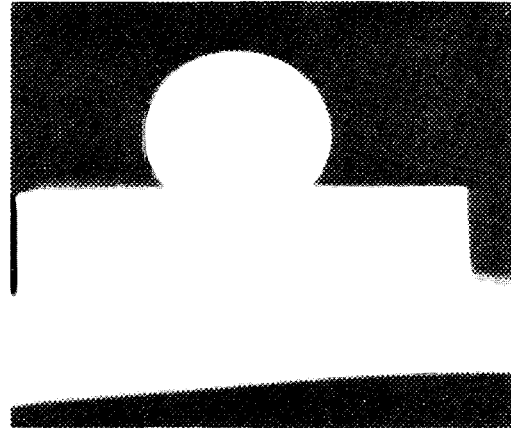
When tests were performed in an argon atmosphere, the same procedure was used except that the system was backfilled with high-purity argon when the muffle temperature reached 800°C (500°C for the aluminum tests).

The wetted specimens were removed from the furnace and mounted, sectioned, and polished for metallographic examination. The mounting and polishing technique employed is described in the Appendix. Examination of the mounted specimens was performed in both the as-polished and polished-and-etched conditions, using both bright-field and polarized-light illumination.

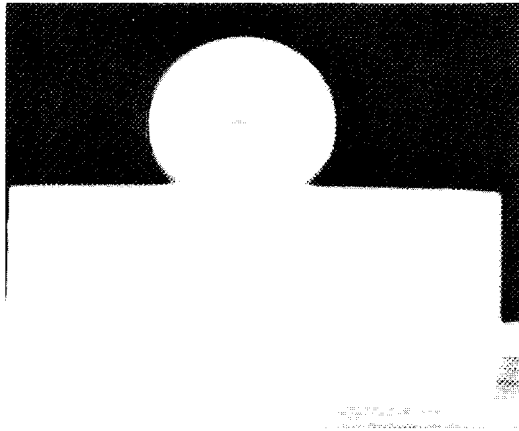
The photographs of the liquid drops were printed on high-contrast matte paper to obtain the greatest detail and allow pencil marking of the prints. Representative photographs are shown in Figures 4 through 11. These particular pictures of the molten-metal drop were taken after a period of 150 seconds had elapsed at the indicated testing temperature. It is obvious from these composite figures that the

Unclassified
Y-49198

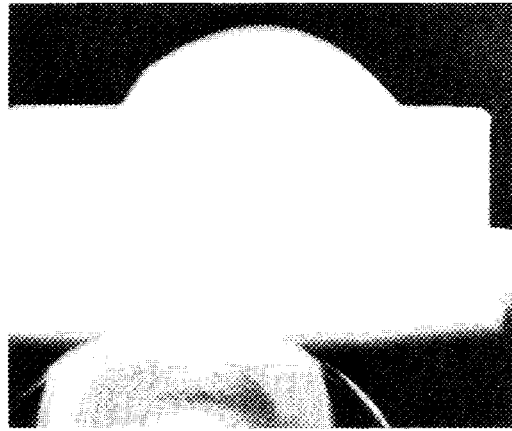
(a) Vacuum - 1010°C



(b) Vacuum - 1060°C



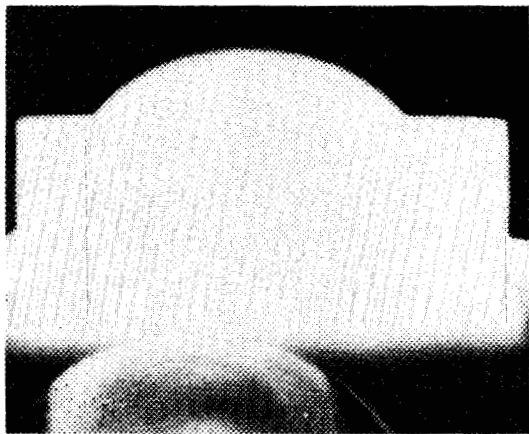
(c) Argon - 1010°C



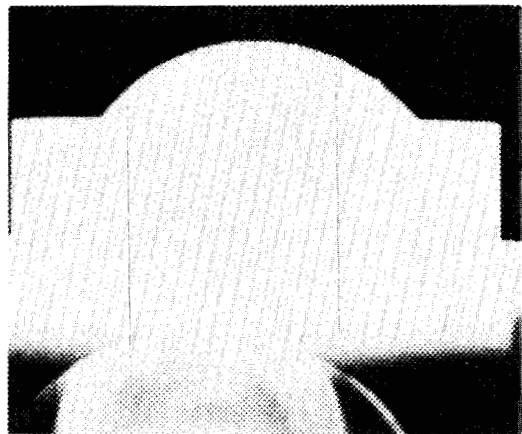
(d) Argon - 1060°C

Figure 4. Sessile drop of silver on beryllium pad at 1010 and 1060°C in vacuum and argon atmospheres. 7X.

Unclassified
Y-49199

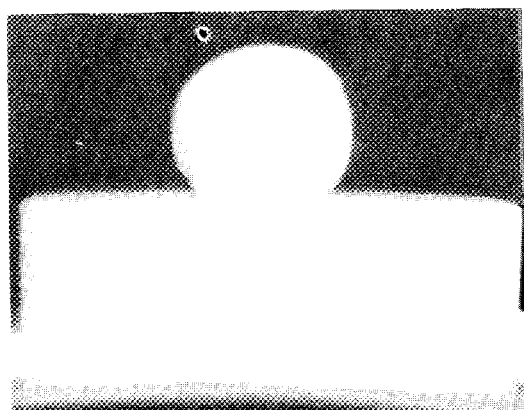


(a) Argon - 1070°C

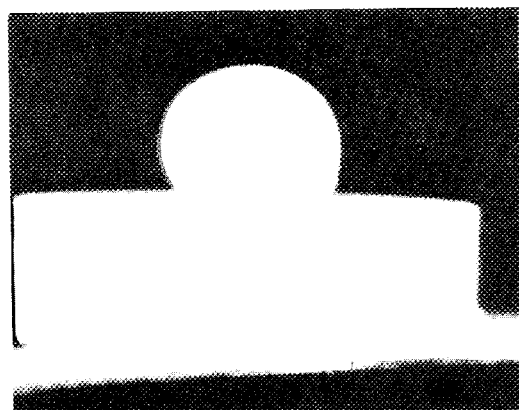


(b) Vacuum - 1070°C

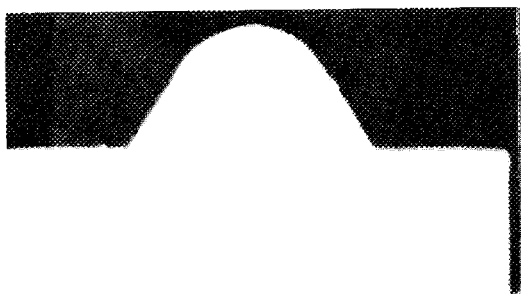
Figure 5. Sessile drop of gold on beryllium pad at 1070°C in argon and vacuum atmospheres. 7X.

Unclassified
Y-49200

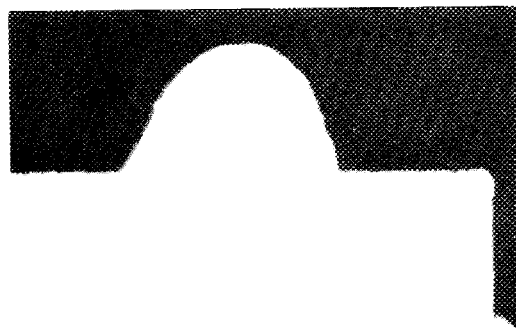
(a) Vacuum - 1108°C



(b) Vacuum - 1133°C

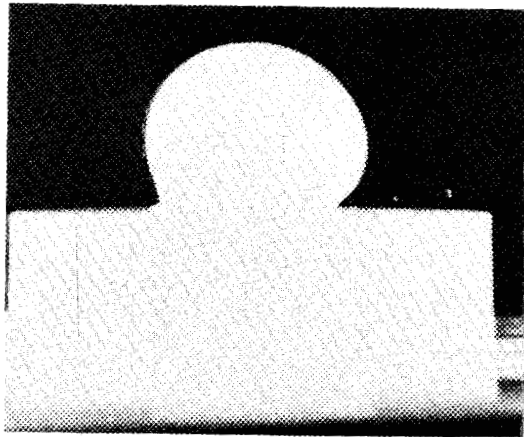


(c) Argon - 1108°C

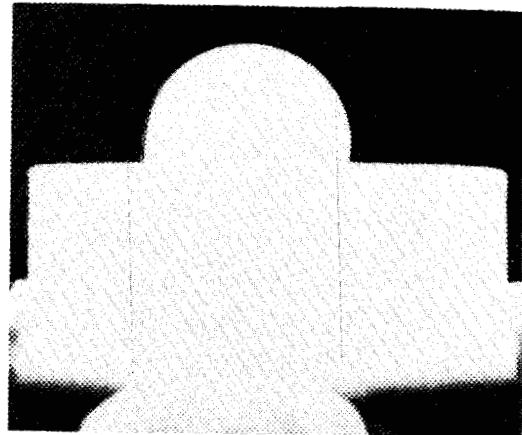


(d) Argon - 1133°C

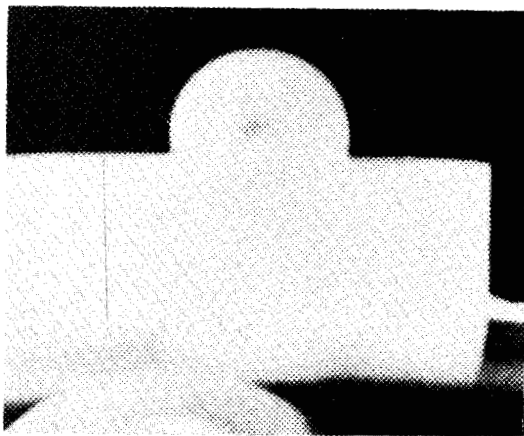
Figure 6. Sessile drop of copper on beryllium pad at 1108 and 1133°C in vacuum and argon atmospheres. 7X.

Unclassified
Y-49201

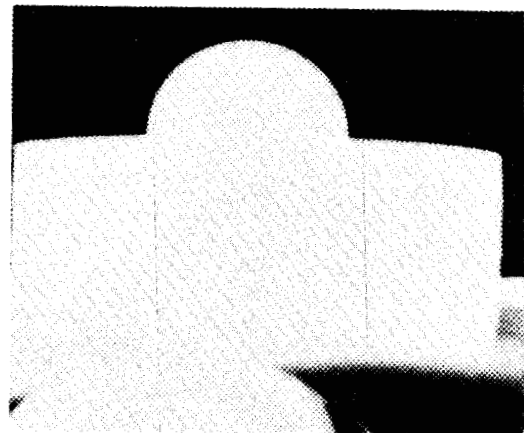
(a) Vacuum - 1000°C



(b) Vacuum - 1050°C

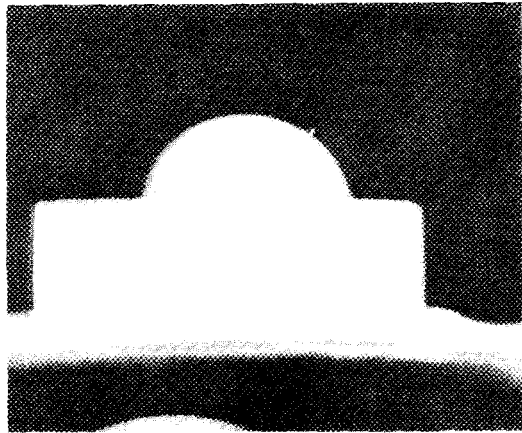


(c) Argon - 1000°C

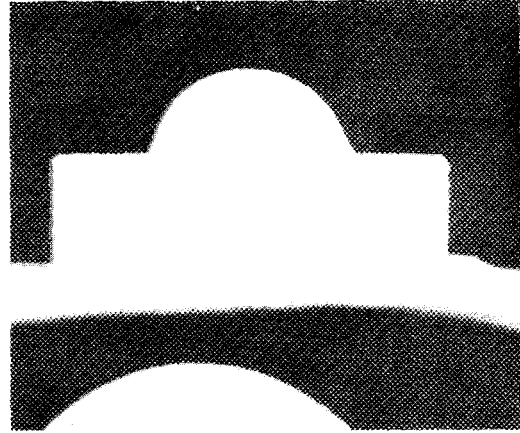


(d) Argon - 1050°C

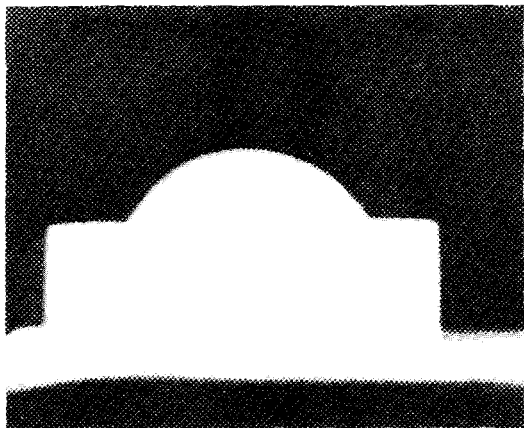
Figure 7. Sessile drop of germanium on beryllium pad at 1000 and 1050°C in vacuum and argon atmospheres. 7X.

Unclassified
Y-49202

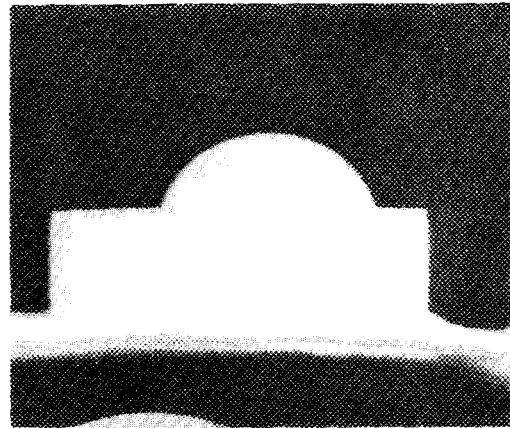
(a) Vacuum - 980°C



(b) Vacuum - 1030°C

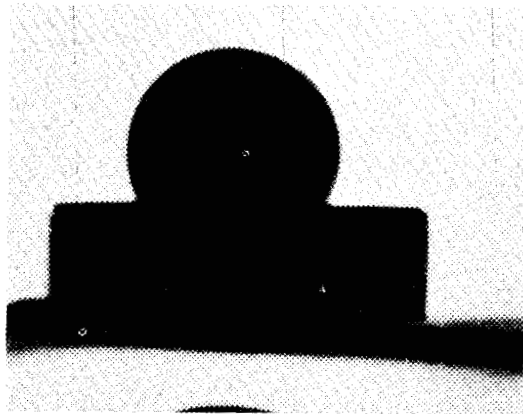


(c) Argon - 980°C

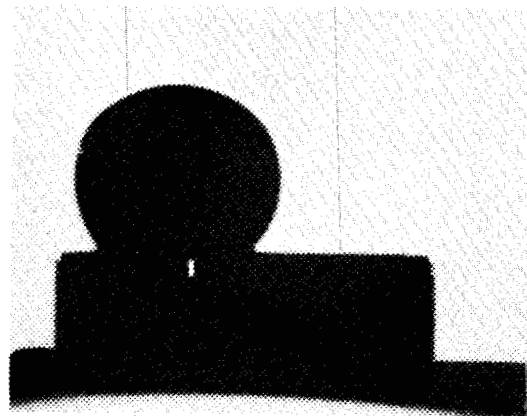


(d) Argon - 1030°C

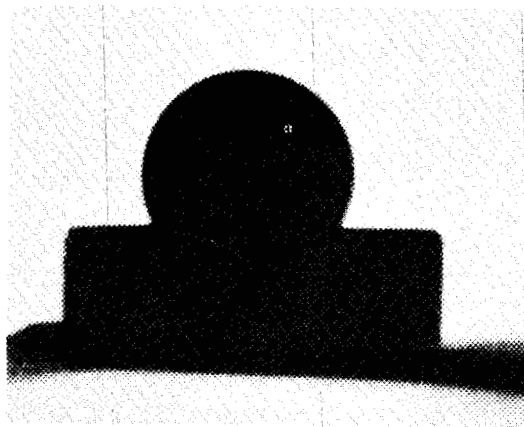
Figure 8. Sessile drop of palladium-2.1 weight per cent beryllium alloy on beryllium pad at 980 and 1030°C in vacuum and argon atmospheres. 7X.

Unclassified
Y-49203

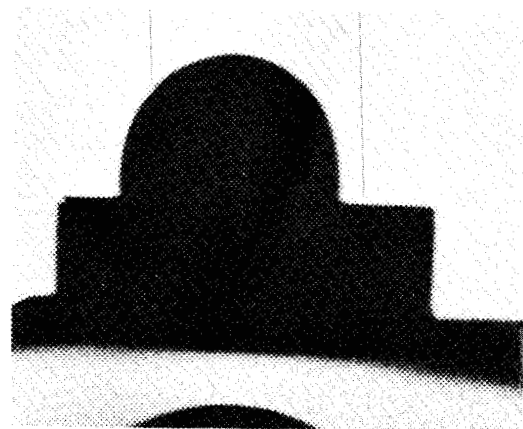
(a) Vacuum - 710°C



(b) Vacuum - 760°C

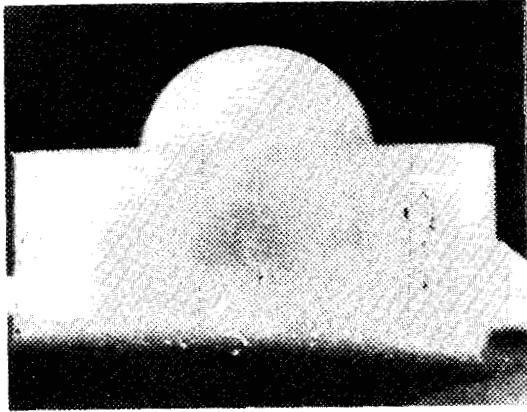


(c) Argon - 710°C



(d) Argon - 760°C

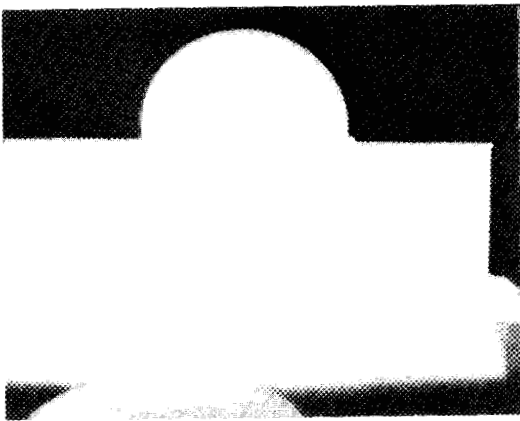
Figure 9. Sessile drop of aluminum on beryllium pad at 710 and 760°C in vacuum and argon atmospheres. 7X.

Unclassified
Y-49204

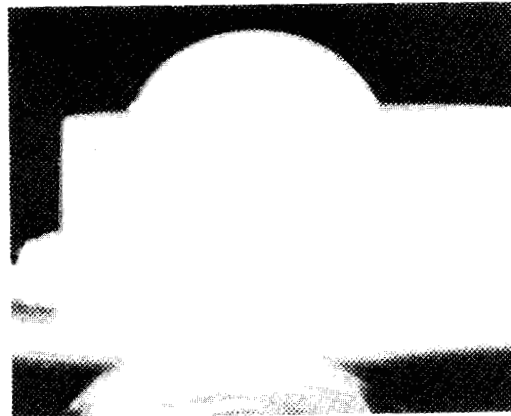
(a) Vacuum - 1030°C



(b) Vacuum - 1080°C

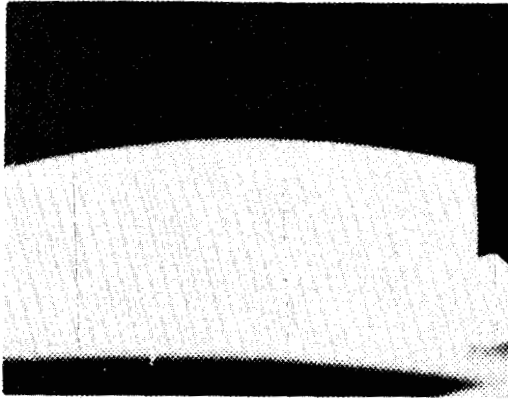


(c) Argon - 1030°C



(d) Argon - 1080°C

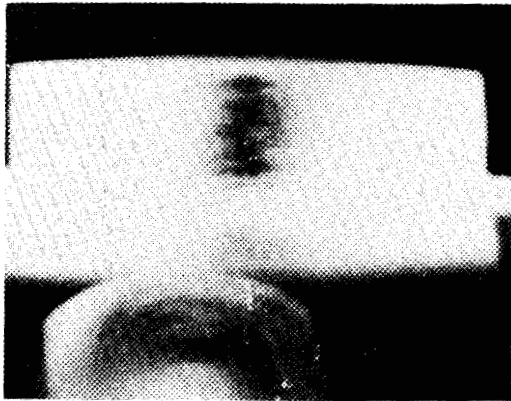
Figure 10. Sessile drop of zirconium-5 weight per cent beryllium alloy on beryllium pad at 1030 and 1080°C in vacuum and argon atmospheres. 7X.

Unclassified
Y-49205

(a) Vacuum - 1075°C



(b) Vacuum - 1125°C



(c) Argon - 1075°C



(d) Argon - 1125°C

Figure 11. Sessile drop of titanium-6 weight per cent beryllium alloy on beryllium pad at 1075 and 1125°C in vacuum and argon atmospheres. 7X.

increase in temperature generally produces increased wetting of the beryllium surface by the sessile drop. The effect of atmosphere on beryllium wettability appears to vary with the system in question.

Contact angle measurements were made on the photographs with a protractor. The sessile-drop contact angle was taken to be that angle between the line tangent to the sessile drop at the point of contact with the beryllium pad and the horizontal surface of the beryllium. Since the contact angle is always measured through the liquid phase, a contact angle of 0 degrees indicates complete wetting while a contact angle of 180 degrees indicates no wetting. The contact angle for each temperature and atmosphere was recorded for each time interval at which photographs had been taken.

The final phase of the study consisted of the calculation of the surface tensions. Only those molten metals which indicated, by metallographic examination, little or no interfacial reactions were used in these calculations. The photographs of the test samples taken at the 150-second time interval were assumed to represent equilibrium and were used for the surface tension calculations.

The determination of the surface tension by the sessile-drop method was accomplished by equating the hydrostatic pressure of the liquid at any point on its surface to the excess pressure due to the curvature and tension of the surface at the point in question. The actual calculation is therefore performed using the dimensions of the molten-metal drop as it rests on the beryllium metal. The shape of

the sessile drop depends on the equilibrium existing between the forces of surface energy and of gravity. The relationships employed were developed by Bashforth and Adams (21), and the calculations utilized data from table prepared by them. A discussion of this method and a sample calculation of the liquid and interfacial surface tensions, the work of adhesion, and the interfacial spreading coefficient are presented in the Appendix.

CHAPTER VI

RESULTS AND DISCUSSION

I. QUALITATIVE DISCUSSION OF CONTACT ANGLE MEASUREMENTS

The data resulting from the contact angle measurements of the liquid metals at test temperatures are presented in Table III. The measurements were recorded for various temperatures, times, and atmospheres. The methods and criteria by which the data were obtained and analyzed, respectively, are described in Chapter V.

Although during the testing period fluctuations in angle were noted, the contact angles were observed to decrease with increasing time at test temperature. This behavior is reflected in the data of Table III. The fluctuations are possible due to alloying effects in that, as alloying progresses, composition and temperature variations will change the interfacial energies.

These data provide a means of comparison of the wettability on beryllium of the liquid metals under investigation. If one assumes wetting for contact angles less than 90 degrees and nonwetting for angles greater than 90 degrees, then these data permit qualitative separation of the systems into these two classes. Gold, palladium-2.1 weight per cent beryllium, and titanium-6 weight per cent beryllium were found to wet beryllium at both temperatures and in both argon and vacuum atmospheres. The zirconium-5 weight per cent beryllium alloy wets beryllium in vacuum at both temperatures. This alloy, as

TABLE III
VALUES OF CONTACT ANGLES FOR VARIOUS TIMES, TEMPERATURES, AND ATMOSPHERES

System	Temperature (°C)	Atmosphere	Contact Angle for Elapsed Time (deg)				
			0 sec	15 sec	45 sec	90 sec	150 sec
Silver	1010	vacuum	142.3	141.1	140.6	141.2	140.2
	1060	vacuum	135.4	135.6	131.4	133.2	127.9
	1010	argon	148.1	148.9	150.7	147.3	143.4
	1060	argon	61.0	59.9	57.2	54.4	52.6
Gold	1070	vacuum	58.6	58.0	57.2	55.7	54.6
	1070	argon	57.3	56.6	57.9	56.9	55.8
Copper	1108	vacuum	129.0	128.5	124.2	124.1	123.6
	1133	vacuum	126.6	122.5	121.8	120.0	120.0
	1108	argon	Extreme Base Metal Solution				
	1133	argon	Extreme Base Metal Solution				
Germanium	1000	vacuum	145.5	145.3	144.3	143.7	143.6
	1050	vacuum	102.9	100.0	100.9	96.1	95.4
	1000	argon	99.3	99.6	98.9	98.2	97.1
	1050	argon	89.2	89.2	88.9	87.1	87.1
Pd-2.1 wt % Be	980	vacuum	77.0	74.0	73.2	70.8	69.9
	1030	vacuum	74.2	73.2	68.7	66.5	65.6
	980	argon	77.2	76.5	76.0	75.0	72.7
	1030	argon	70.2	63.1	61.7	57.2	57.2

TABLE III (continued)

System	Temperature (°C)	Atmosphere	Contact Angle for Elapsed Time (deg)				
			0 sec	15 sec	45 sec	90 sec	150 sec
Aluminum	710	vacuum	155.1	154.1	151.3	146.6	142.0
	760	vacuum	140.0	138.8	136.6	134.1	132.0
	710	argon	146.2	139.6	130.5	120.1	116.6
	760	argon	108.2	106.6	102.3	100.0	99.9
Zr-5 wt % Be	1030	vacuum	88.0	85.6	83.9	81.8	80.9
	1080	vacuum	69.8	67.7	67.3	66.5	64.7
	1030	argon	101.4	98.8	99.2	98.3	96.2
	1080	argon	83.6	84.2	84.9	82.4	79.7
Ti-6 wt % Be	1075	vacuum	15.8	14.8	14.5	14.0	13.2
	1125	vacuum	14.2	13.4	12.1	11.2	10.7
	1075	argon	13.4	12.0	11.9	9.7	8.6
	1125	argon	10.0	7.9	7.8	6.8	5.6

well as silver and germanium, did not wet when tested in argon atmospheres at the lower temperature. It was found, however, that an increase of 50°C resulted in wetting. Aluminum exhibited a nonwetting behavior at both temperatures and in both atmospheres. Copper was observed to be nonwetting at both temperatures, but underwent extensive alloying with the solid beryllium at these temperatures.

From these data it appears that the binary alloys have the greatest tendency to wet beryllium. Although differences in wetting behavior were observed for the vacuum and argon conditions, no general trend was established. The increase in testing temperature was generally observed to improve wetting, although in some cases the increased temperature initiated or accelerated reaction with the beryllium.

II. RESULTS OF METALLOGRAPHIC ANALYSIS

It must be recognized that when a metal is allowed to melt on a solid surface some degree of reaction will occur at the solid-liquid interface.

The extent to which this reaction occurs depends on the system in question, particularly the mutual solubility of each component for the other and the wetting behavior of the resulting alloy formed. Normally, interfacial energy studies involve interactions which are confined to essentially the interface. When high temperatures such as those incorporated in this study are used, the diffusion of components across this interface becomes prominent. This diffusion

produces layers each of which is one of the possible phases in the system. Extended diffusion tends to give a liquid saturated with beryllium at the interface and in contact with that solid phase richest in the original liquid metal. Further changes then depend upon solid-state diffusion through these layers; this stage is frequently slow enough to consider the system in psuedoequilibrium.

As a consequence, it is necessary to utilize the equilibrium diagram for each combination with beryllium in analyzing the wetting behavior in each case. This has been done in the discussion of the results of the metallographic studies which follows. From these studies, the extent of alloying could be determined and a basis established for the usefulness of carrying out surface tension calculations.

Silver-Beryllium

The silver-beryllium alloy system is represented by the equilibrium diagram of Figure 12 (22). When pure silver is in contact with beryllium at 1010°C a concentration gradient is established in the liquid phase with a maximum concentration of 2.3 weight per cent beryllium (Figure 12). An examination of the microstructure of the interface revealed a reaction zone in which molten silver had penetrated the grain boundaries of the beryllium. The grain-boundary penetration is illustrated in Figure 13. Penetration has proceeded to the point of leaving pure beryllium islands floating in the liquid silver-beryllium alloy. According to the silver-beryllium equilibrium

Unclassified
Y-49253

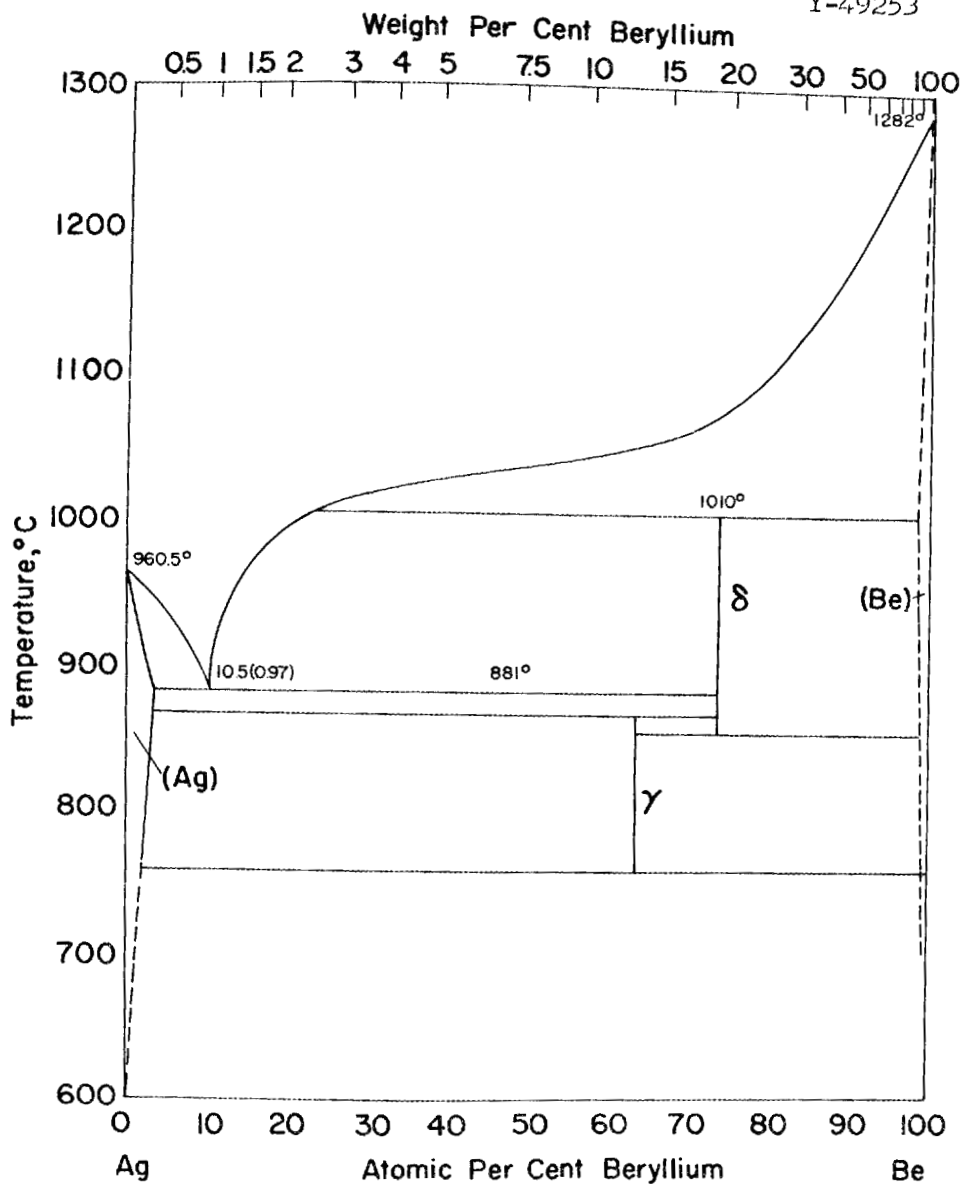


Figure 12. The silver-beryllium equilibrium diagram.
(Hansen, M., Constitution of Binary Alloys, McGraw-Hill, New York, 1958.)

Unclassified
R-10576

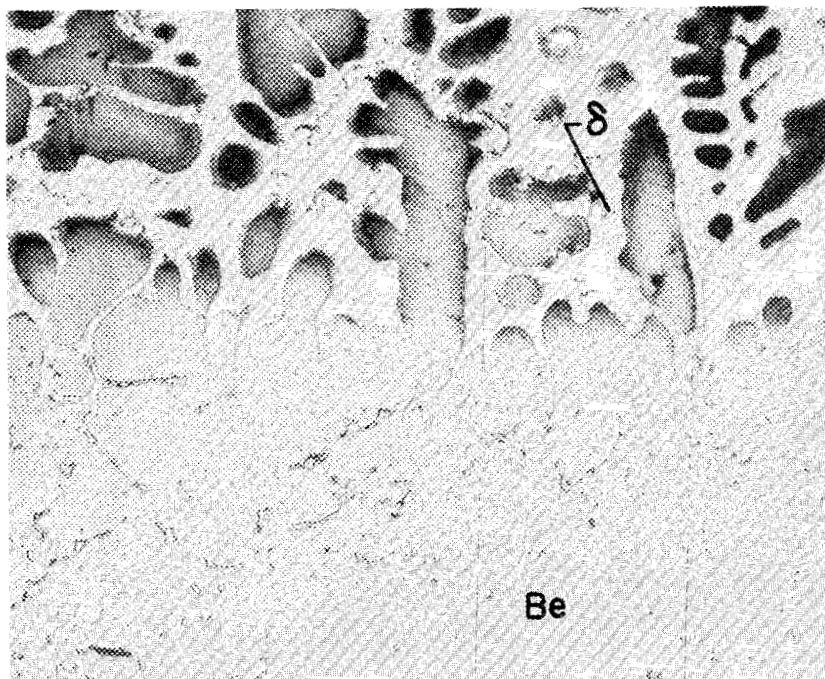


Figure 13. Interface of silver wetting test showing grain-boundary attack of silver on beryllium in a vacuum atmosphere at 1010°C. Unetched. 500X.

diagram, the delta phase should precipitate on cooling and this is observed to occur along the boundary between the liquid and solid phases. The lighter areas surrounding the solid beryllium islands in Figure 13, page 36, are believed to be the delta phase.

Higher temperatures (1060°C) produced a greater reaction zone. This probably resulted from more rapid diffusion and the ability of the liquid to contain as much as 17.5 weight per cent beryllium. On cooling from this temperature, the precipitation of alpha beryllium occurs initially and is followed by the precipitation of the delta phase at 1010°C. From this point the system behaves in a similar manner to the low-temperature test.

The only noticeable difference in the wetting tests conducted in argon and those conducted in vacuum at either temperature was the degree of beryllium reaction. While beryllium reaction was found to be greater at 1060°C in both argon and vacuum atmospheres, more reaction was found in the argon atmosphere tests. The extent of reaction at 1060°C in vacuum is illustrated in Figure 14. Here the penetration is greater than 50 per cent of the beryllium pad thickness. Note the dendritic structure of the alloy drop.

Gold-Beryllium

The extensive reaction of pure gold with beryllium restricted testing to 1070°C, approximately 7 degrees above the melting point of gold. The partial equilibrium diagram for this system is presented in Figure 15 (22). Metallographic examination of both the vacuum and

Unclassified
R-10577

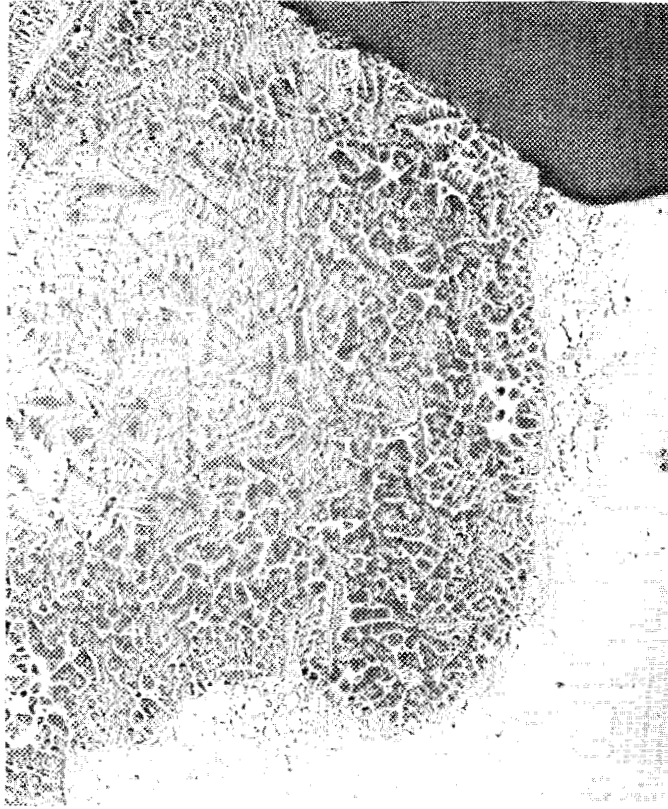


Figure 14. Silver penetrating beryllium metal at 1060°C in a vacuum atmosphere. Unetched. 50X.

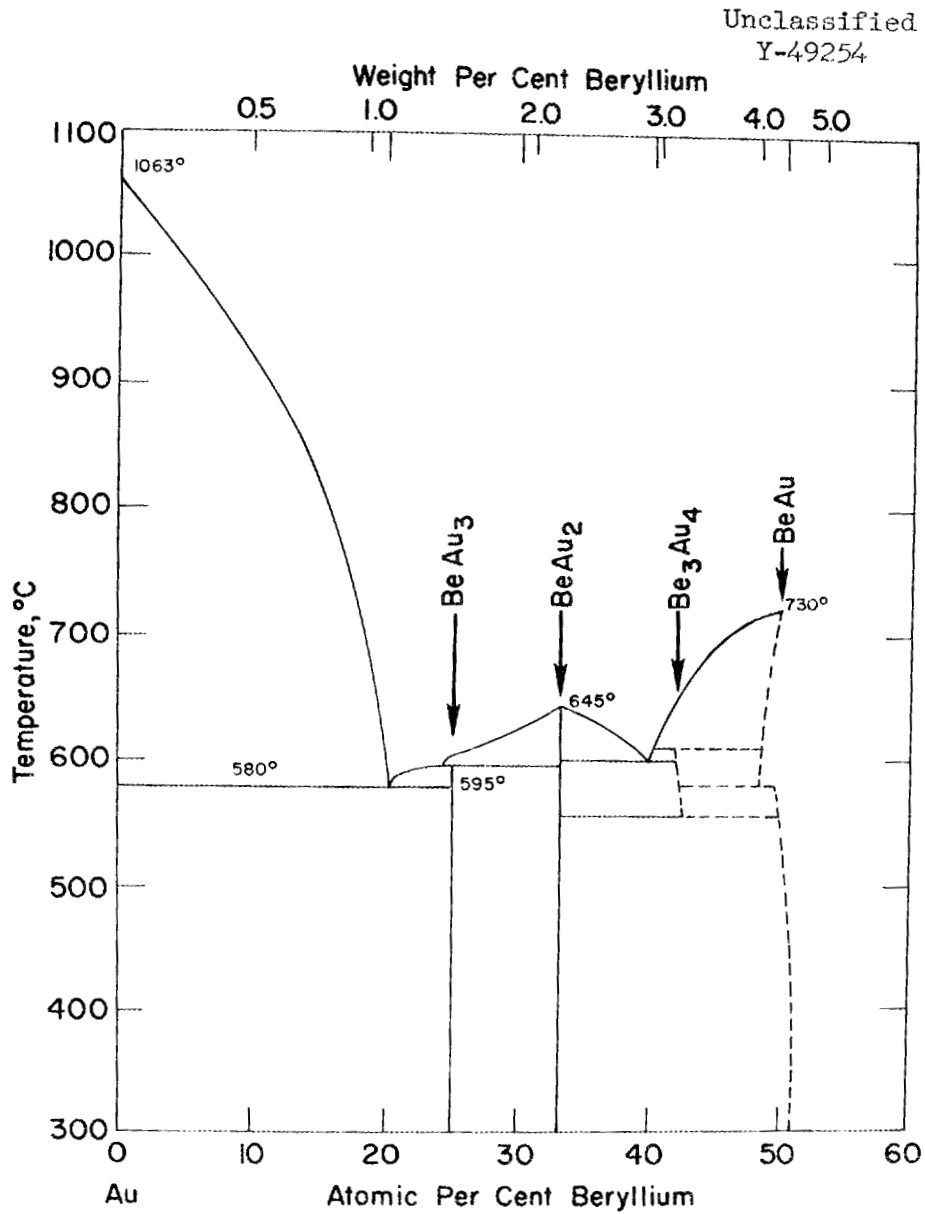


Figure 15. The gold-beryllium equilibrium diagram.
(Hansen, M., Constitution of Binary Alloys, McGraw-Hill, New York, 1958.)

argon tests revealed extreme alloying, as illustrated in Figure 16. Metallographic examination revealed a second phase, shown in Figure 17, which is probably one of the intermetallic compounds shown in the gold-beryllium equilibrium diagram (Figure 15, page 39); no positive identification was possible. No particular difference in the microstructure of the argon and vacuum tests was observed metallographically.

Copper-Beryllium

The equilibrium diagram for the copper-beryllium systems is shown in Figure 18 (22). Low-temperature vacuum tests resulted in a small amount of reaction with beryllium while at the same temperature in argon extreme reaction occurred. This difference is shown in Figure 19(a) and (b). In the case of the vacuum test, only the reaction zone shows noticeable alloying; while in the argon test, alloying was observed throughout the liquid phase. According to the copper-beryllium equilibrium diagram, the delta phase should initially precipitate on cooling until the liquid has been depleted of beryllium to the point that the beta phase forms. This was observed to occur by the initial formation of the delta phase that is believed to be the dendritic growth seen in the reaction zones of Figure 19. Further cooling formed the lighter matrix that is assumed to be either beta phase or some decomposition product of this phase.

The microstructure of the drop above the low-temperature vacuum reaction zone of Figure 19(a) is shown in Figure 20. The dendrites are assumed to be the alpha phase since the beryllium concentration

Unclassified
R-10583



Figure 16. Gold penetration of beryllium metal at 1070°C in a vacuum atmosphere. Unetched. 50X.

Unclassified
Y-48067



Figure 17. The microstructure of the gold drop on beryllium at 1070°C in a vacuum atmosphere. Etchant: aqua regia. 500X.

Unclassified
Y-49255

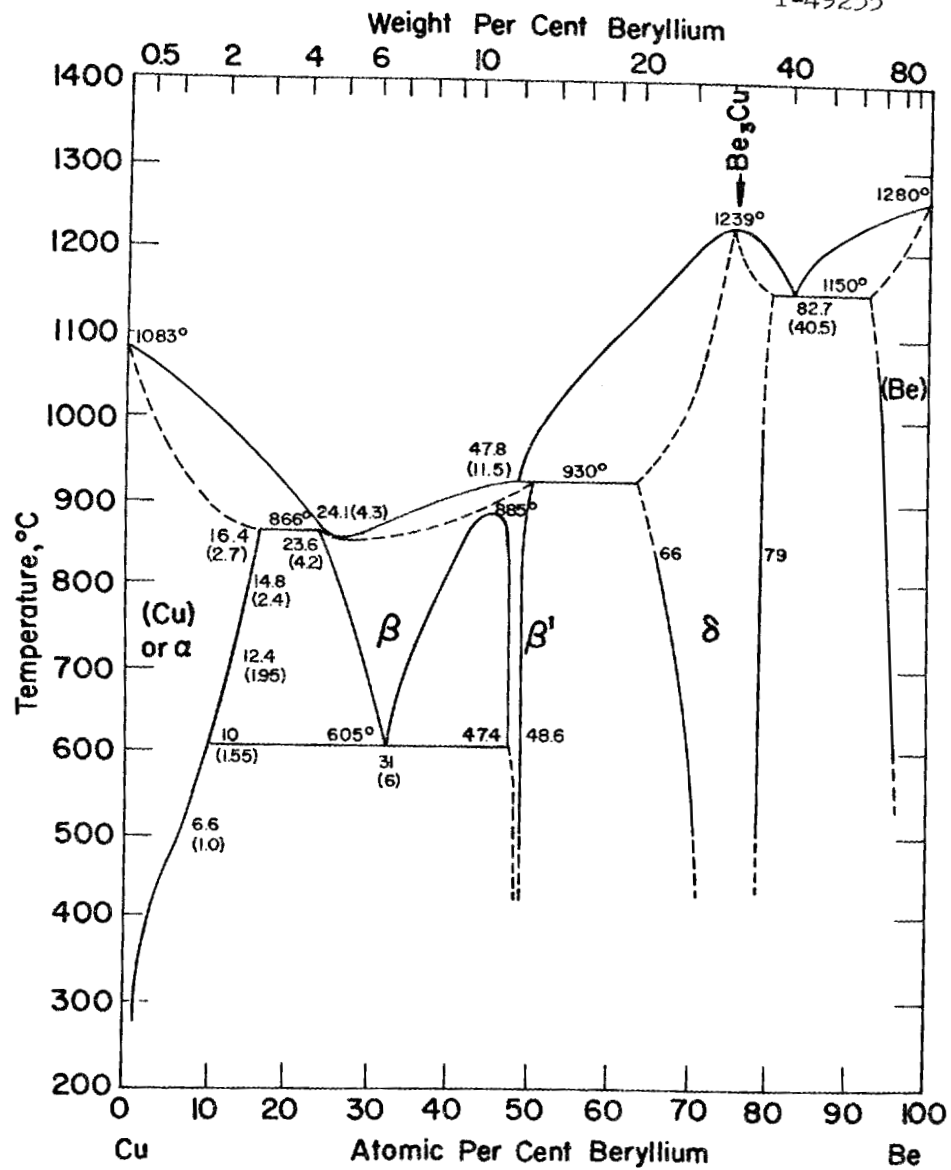
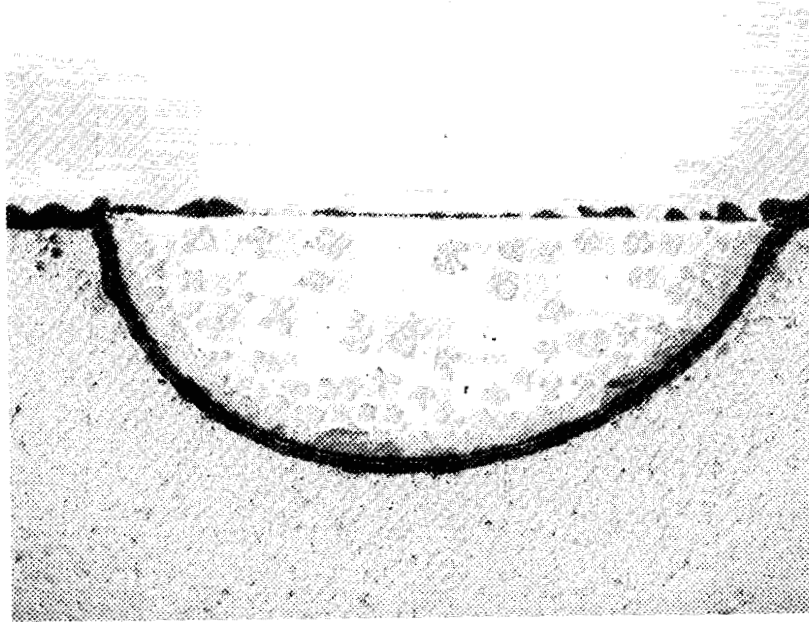


Figure 18. The copper-beryllium equilibrium diagram.
(Hansen, M., Constitution of Binary Alloys, McGraw-Hill, New York, 1958.)

Unclassified
R-10597



A.

Unclassified
R-10595



B.

Figure 19. (a) Microstructure of copper drop on beryllium showing interfacial reaction area at 1108°C in a vacuum atmosphere. Unetched. 50X. (b) Microstructure of copper alloying with beryllium at 1108°C in an argon atmosphere. Unetched. 50X.

Unclassified
Y-48113

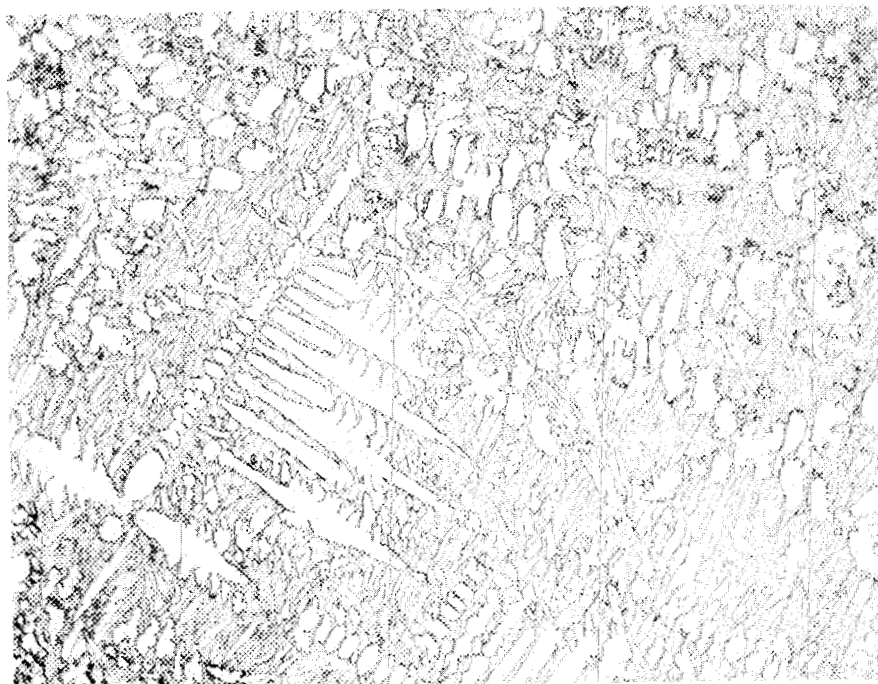


Figure 20. The microstructure of the copper drop at 1108°C in a vacuum atmosphere. Etchant: C_2H_5OH , HCl , $FeCl_3$. 200X.

in the liquid should be lower than that near the interface. Separation of this phase will increase the concentration of the melt to near 4 weight per cent beryllium which will, on further cooling, form beta or some transformation product of beta.

High-temperature experiments (1133°C) revealed that beryllium reaction had proceeded such that complete penetration of the beryllium pad had occurred in both the vacuum and argon tests. Metallographic examination of these samples showed the same microstructure found in the lower temperature tests, with the exception of a reaction band near the pure beryllium-base metal as shown in Figure 21. As seen in Figures 20, page 45, and 21, voids, which probably resulted from rapid diffusion of the small beryllium atom into the two-phase (beta and delta) region, are present in the reaction band. The extent of copper diffusion is assumed to be the interface nearest the beryllium metal. The band structure, shown in Figure 22, is believed to be the result of the formation of the 40.5 weight per cent beryllium-copper eutectic, shown in Figure 19, page 44. Since only a differential of 17°C separates the assumed test temperature (1133°C) and the eutectic temperature (1150°C), temperature inaccuracies could have existed such that the test temperature was truly 1150°C, with the eutectic composition formed by diffusion. One other possibility for this structure to be the beryllium-rich eutectic would be that the eutectic temperature was depressed as a result of the impurities present in the beryllium.

Unclassified
R-10594

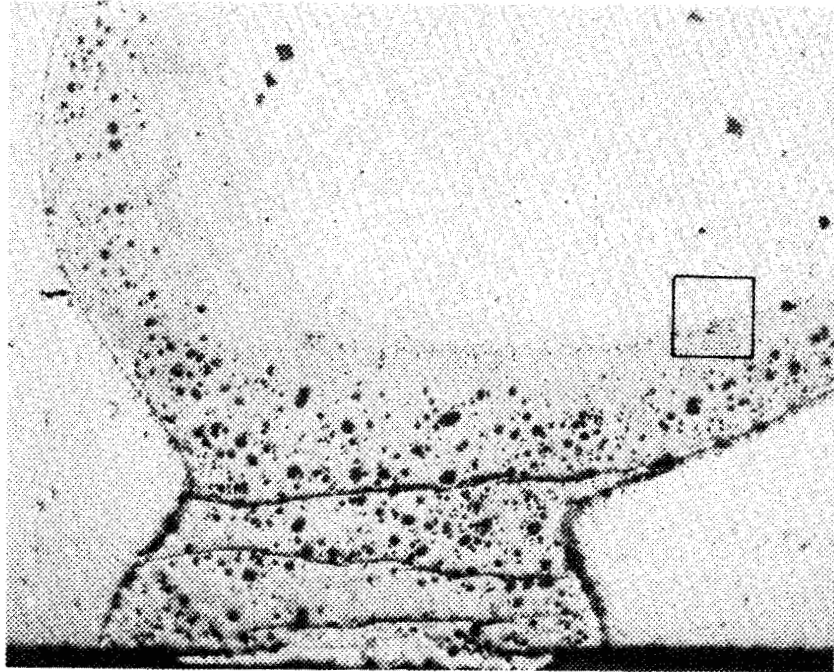


Figure 21. Photomicrograph of the 1133°C copper test in argon showing the reaction zone band near the beryllium metal. Unetched. 50X.

Unclassified
R-10591

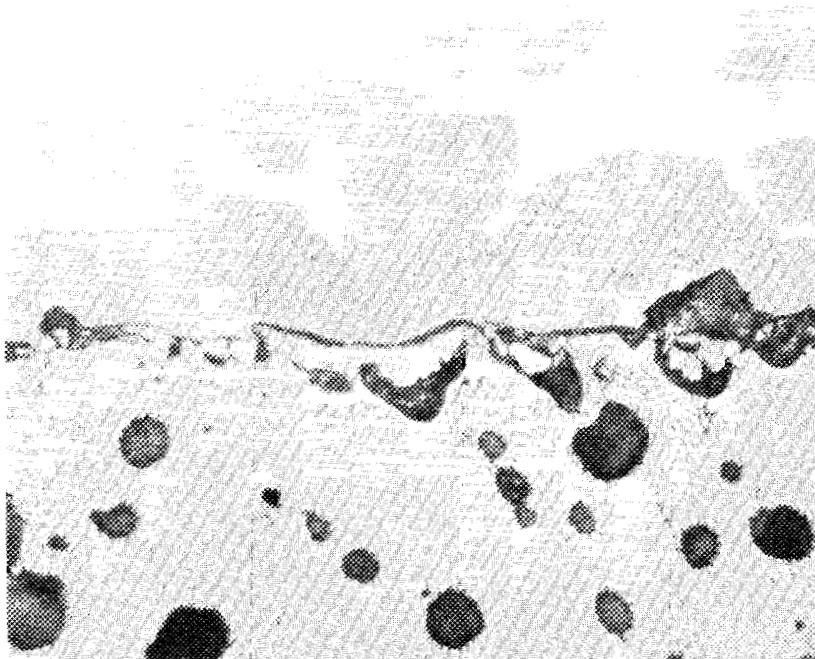


Figure 22. The copper reaction zone band showing its eutectic microstructure. Magnified view of the enclosed area of Figure 21. Unetched. 500X.

Palladium-2.1 weight per cent Beryllium-Beryllium

The partial equilibrium diagram for the palladium-beryllium system is shown in Figure 23 (22). At each test temperature the microstructures were found to be independent of the testing atmosphere and indicated moderate alloying with the beryllium. This small amount of alloying is supported by reference to the palladium-beryllium equilibrium diagram which shows that only an increase of 0.9 weight per cent beryllium in the liquid is necessary to produce saturation.

Representative microstructures of the low- and high-temperature tests are presented in Figures 24 and 25, respectively. The analysis of these microstructures was complicated by the absence of a more complete palladium-beryllium equilibrium diagram. If it is assumed that the liquid was saturated with 3 weight per cent beryllium, the structures seen in both the low-temperature drop (Figure 24) and the upper portion of the high-temperature drop (Figure 25) may be analyzed in terms of the palladium-beryllium equilibrium diagram. The diagram suggests that the islands of these structures are BePd_2 and the matrix is the BePd_3 intermetallic compound. The reaction zone, seen at the interface of the high-temperature tests (Figure 25), exhibited a eutectic-like structure and should be beryllium rich. A photomicrograph of this structure is shown in Figure 26. Since the structure was observed only at the higher temperature, there is probably a eutectic which forms between 980 and 1030°C at compositions above 50 per cent beryllium.

Unclassified
Y-49256

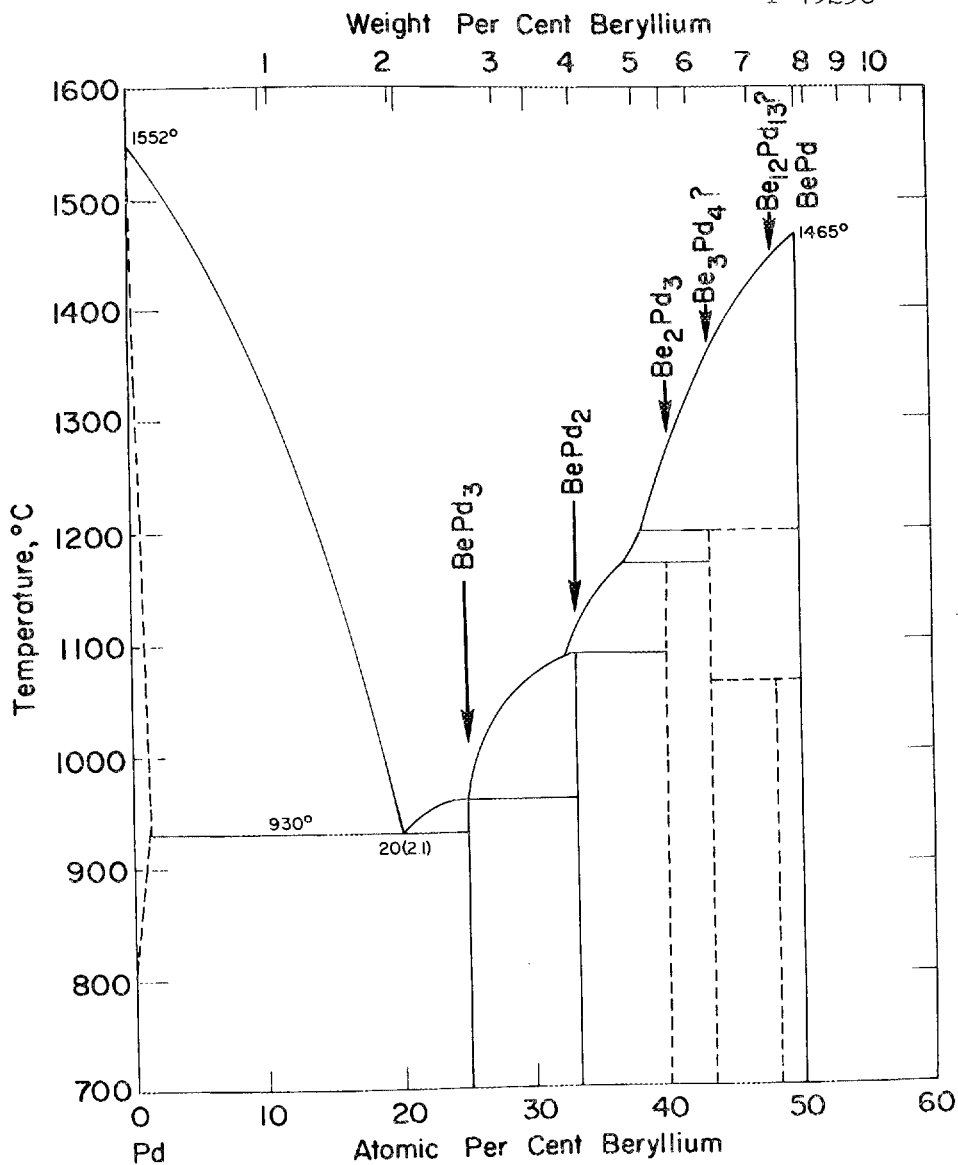


Figure 23. The palladium-beryllium equilibrium diagram.
(Hansen, M., Constitution of Binary Alloys, McGraw-Hill, New York, 1958.)

Unclassified
Y-48117

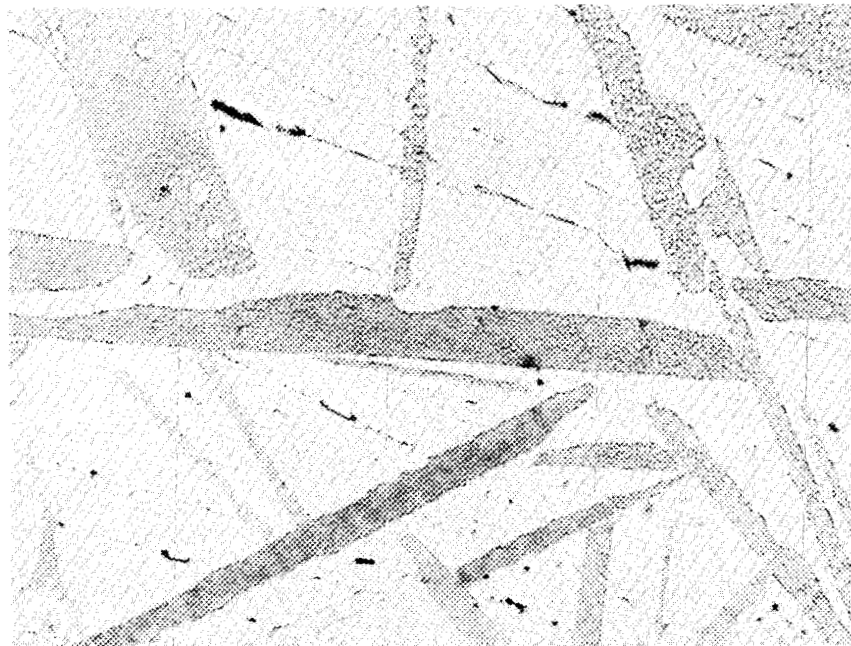


Figure 24. The microstructure of the palladium-2.1 weight per cent beryllium drop representative of tests in both argon and vacuum at 980°C. Etchant: KCN, $(\text{NH}_4)_2\text{S}_2\text{O}_3$. 250X.

Unclassified
Y-48116Palladium-Beryllium
DropInterface Reaction
Zone

Beryllium



Figure 25. The microstructure of the palladium-2.1 weight per cent beryllium sample interface area representative of tests in both argon and vacuum at 1030°C. Polarized light. 150X.

Unclassified
Y-48115

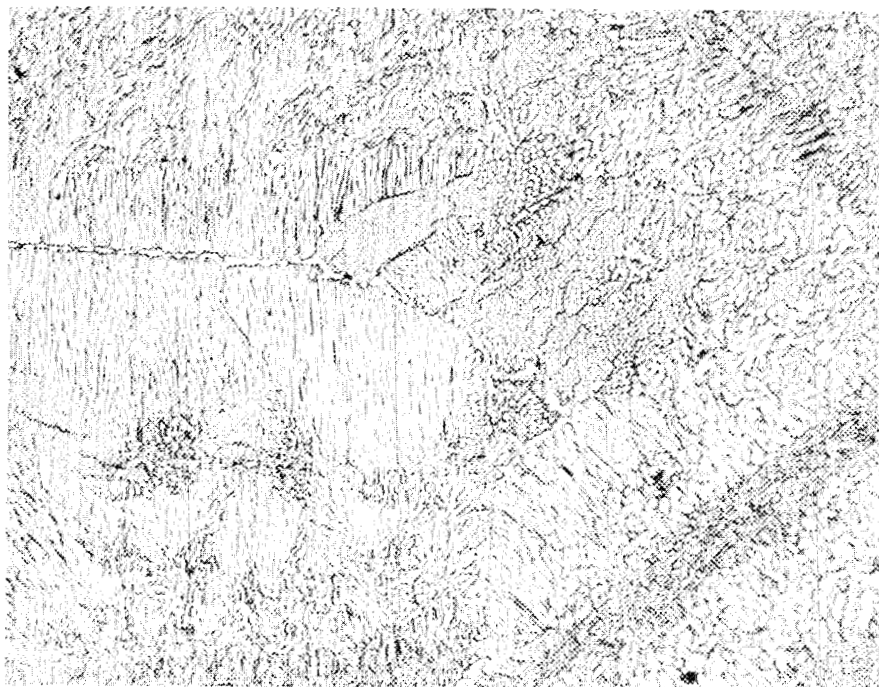


Figure 26. The microstructure of the palladium-beryllium interface area representative of tests in both argon and vacuum at 1030°C. Etchant: aqua regia. 500X.

Germanium-Beryllium

No published equilibrium diagram is currently available for the germanium-beryllium system. Metallographic examination revealed that some interfacial reaction had occurred at 1000 and 1050°C in both argon and vacuum. A representative microstructure is presented in Figure 27. The large, dendritic-like areas in the microstructure were found to be sensitive to polarized light. The matrix phase is probably the germanium-rich terminal solid solution, and the dispersed phase is either an intermediate phase or the terminal beryllium-rich phase.

Aluminum-Beryllium

Metallographic examination of the aluminum-beryllium test samples revealed very little reaction with beryllium at any of the testing conditions. This observation is verified by the aluminum-beryllium equilibrium diagram of Figure 28 that predicts a liquid saturation limit of only 2.5 weight per cent beryllium at 760°C (22). The aluminum-beryllium equilibrium diagram further indicates that on cooling from the temperatures of 710 and 760°C the precipitation of alpha beryllium will occur until the eutectic temperature, 645°C, is reached where final freezing results. A representative aluminum-drop microstructure is presented in Figure 29, showing the eutectic structure. As a result of the limited beryllium reaction of this liquid, further surface energy analysis was performed. The results of this analysis are presented subsequently.

Unclassified
Y-48068

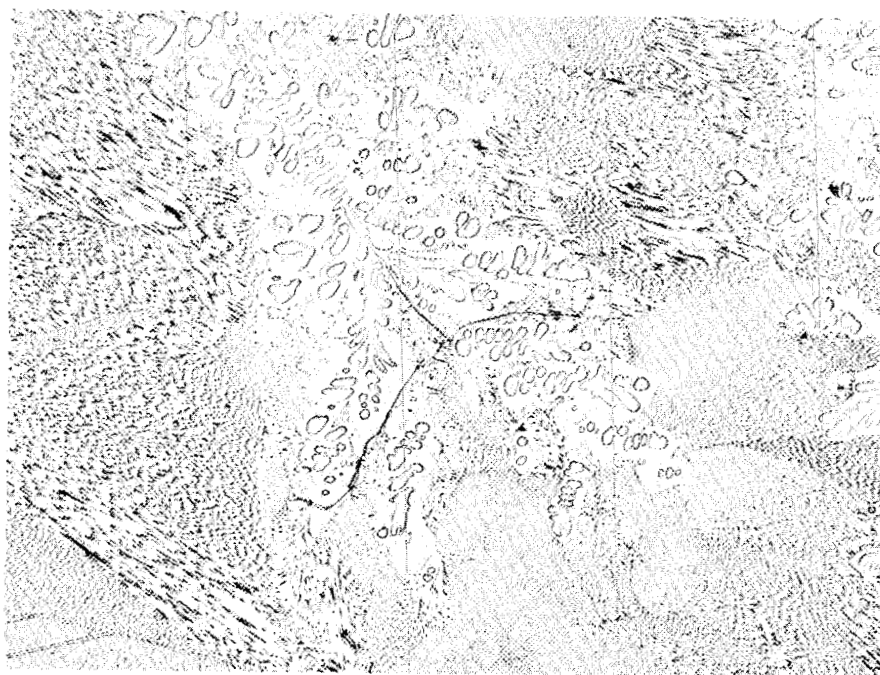


Figure 27. Representative microstructure of the germanium drop at 1000°C in a vacuum atmosphere. Etchant: $\text{HC}_2\text{H}_3\text{O}_2$, HF, HNO_3 . 150X.

Unclassified
Y-49257

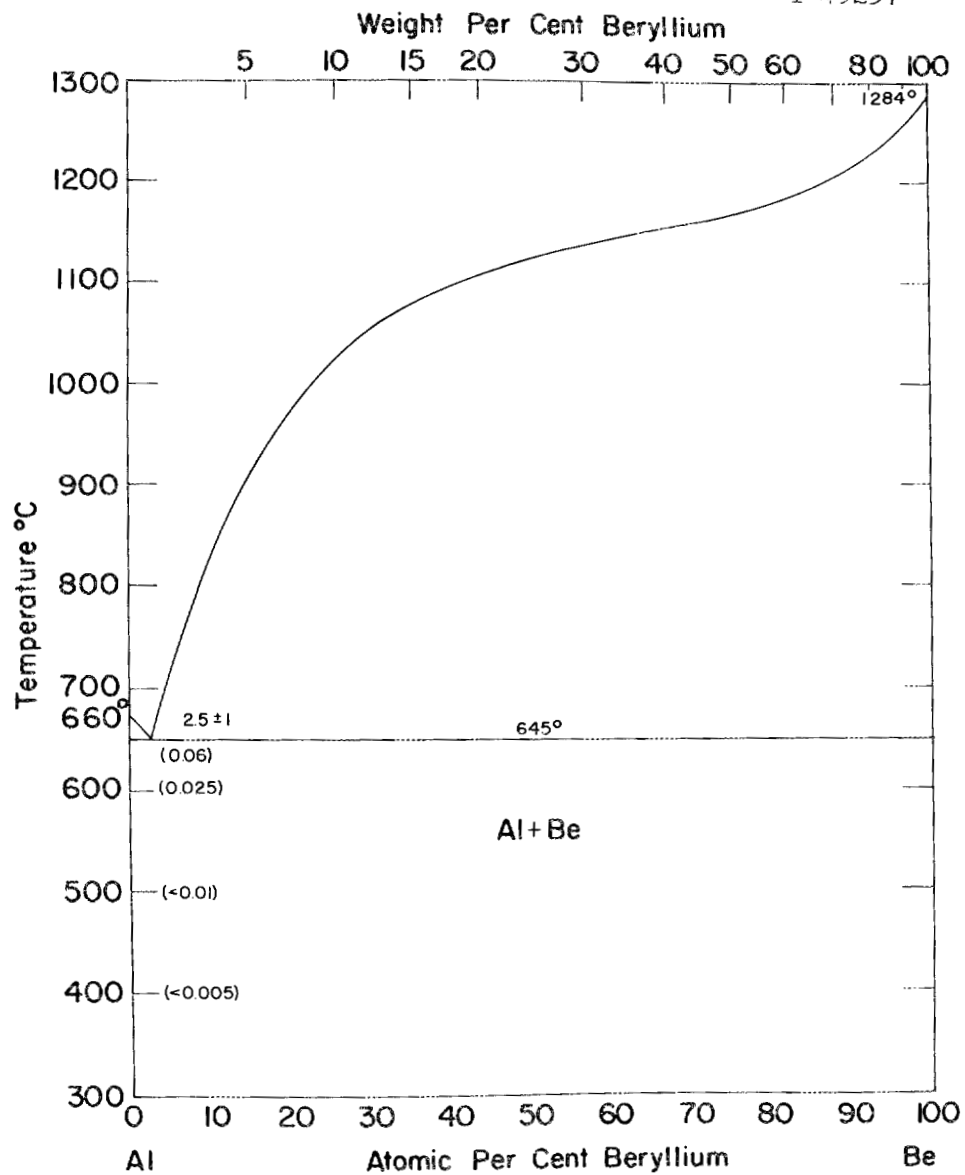


Figure 28. The aluminum-beryllium equilibrium diagram.
(Hansen, M., Constitution of Binary Alloys, McGraw-Hill, New York, 1958.)

Unclassified
Y-48114

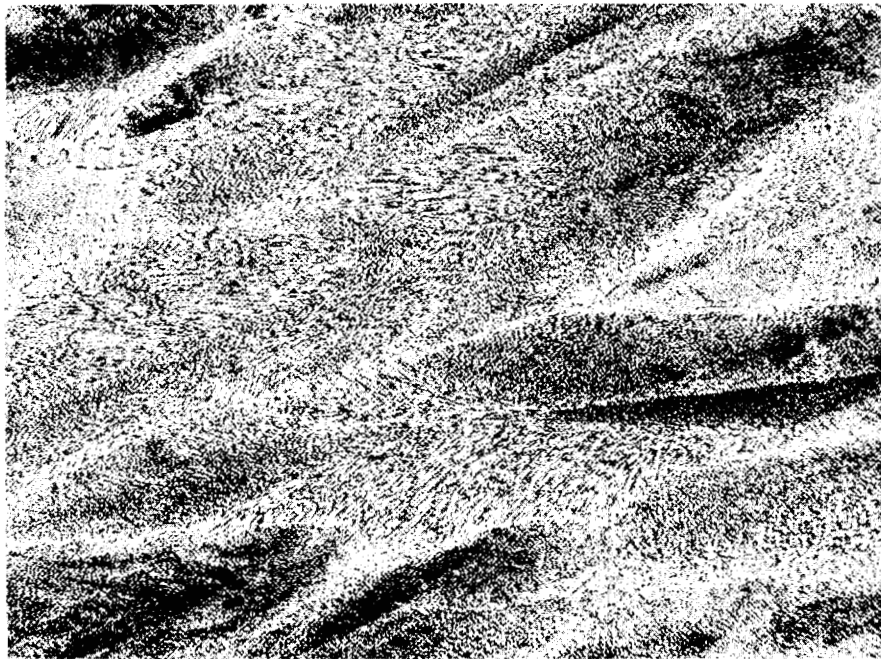


Figure 29. Representative microstructure of the aluminum drop showing the eutectic structure at 760°C in a vacuum atmosphere. Etchant: H₂O, HF, HNO₃, HCl. 150X.

Zirconium-5 weight per cent Beryllium-Beryllium

Metallographic examination of the zirconium-5 weight per cent beryllium eutectic wetting samples revealed no beryllium reaction. According to the zirconium-beryllium equilibrium diagram of Figure 30, only 8 weight per cent beryllium is required to saturate the liquid at 1080°C (23). This accounts for the absence of a reaction area and permits calculation of surface energies.

A representative microstructure of the wetting drop under polarized light is shown in Figure 31. According to the zirconium-beryllium equilibrium diagram, the light, needle-like phase is probably the intermetallic compound, $ZrBe_2$; it is dispersed in the eutectic structure.

Titanium-6 weight per cent Beryllium-Beryllium

The highly wetting titanium-6 weight per cent beryllium alloy was observed metallographically to cause no beryllium reaction at any test condition. The partial equilibrium diagram of the titanium-beryllium system, shown in Figure 32, predicts beryllium solubility in the titanium liquid to be greater than 6 weight per cent, but the exact solubility limit is not known (23). The absence of beryllium reaction permitted further surface energy analysis and the results of this analysis are discussed below. The alloy microstructure contained islands of unidentified intermetallic compounds dispersed in a eutectic matrix. The titanium-beryllium equilibrium diagram predicts the possible existence of as many as five intermetallic compounds, but no

Unclassified
Y-49258

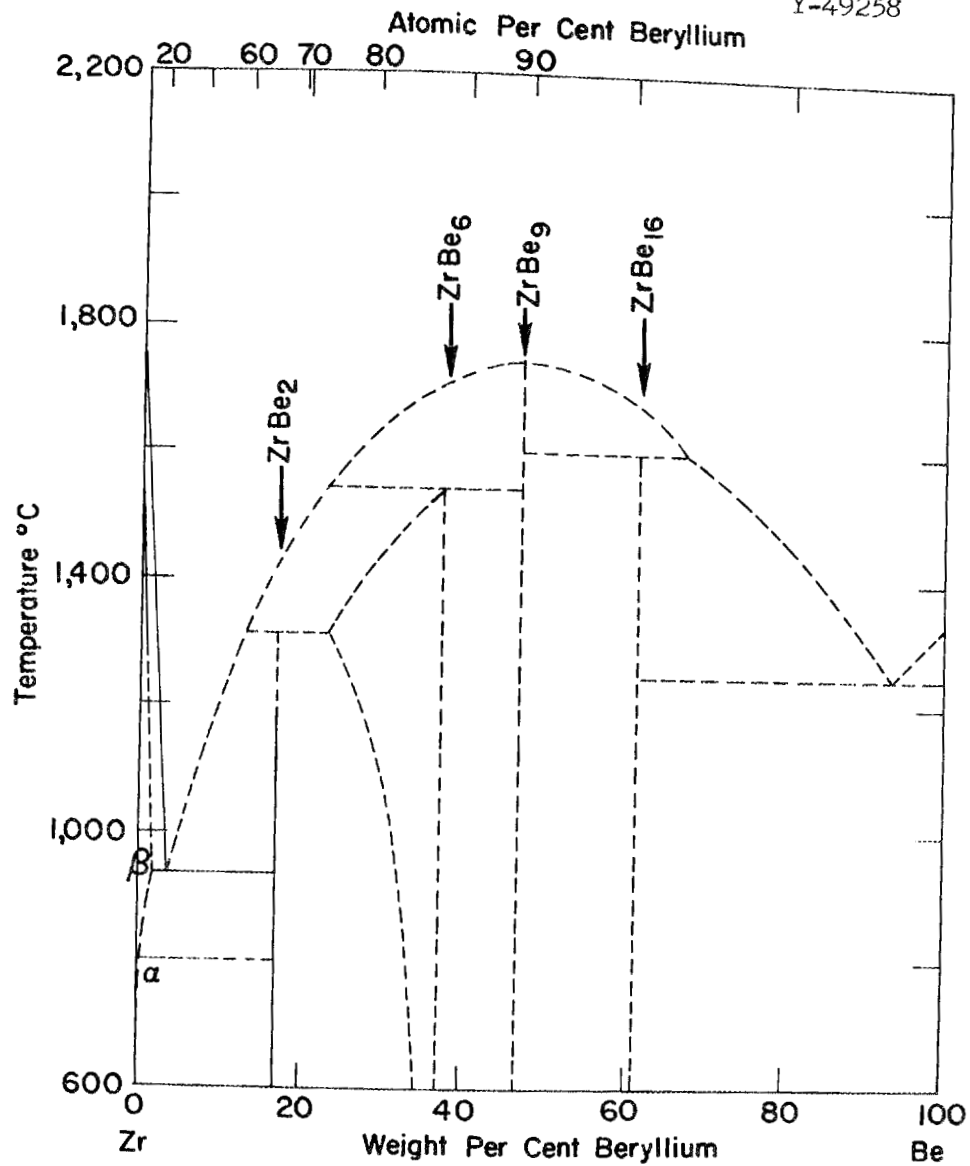


Figure 30. The zirconium-beryllium equilibrium diagram.
(Darwin, G. E., and J. H. Buddary, "Alloys and Compounds," Metallurgy of the Rarer Metals - 7 - Beryllium, Academic Press, New York, 1960, pp. 265-320.)

Unclassified
Y-48066

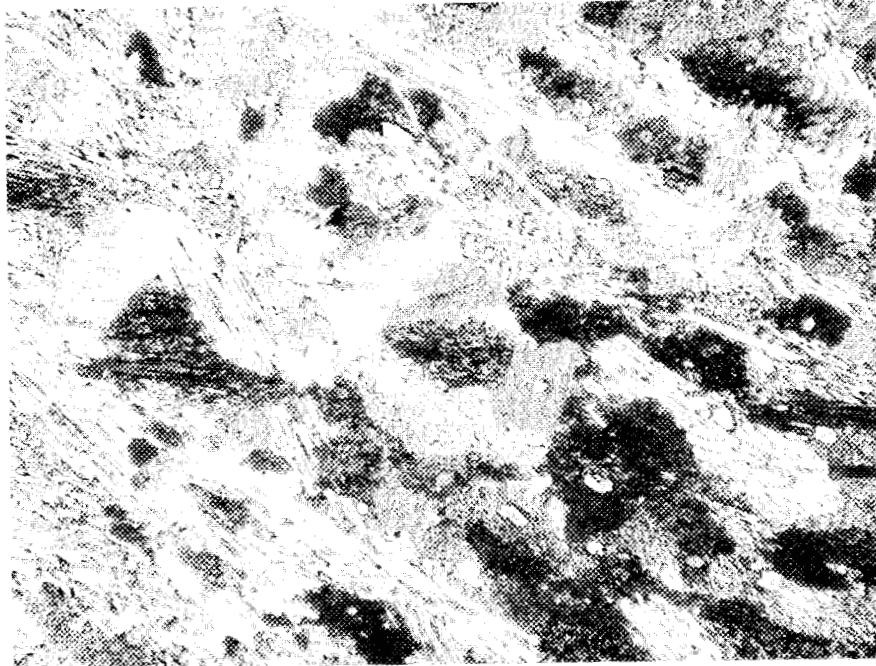


Figure 31. Representative microstructure of the zirconium-5 weight per cent beryllium drop at 1030°C in a vacuum atmosphere. Polarized light. 150X.

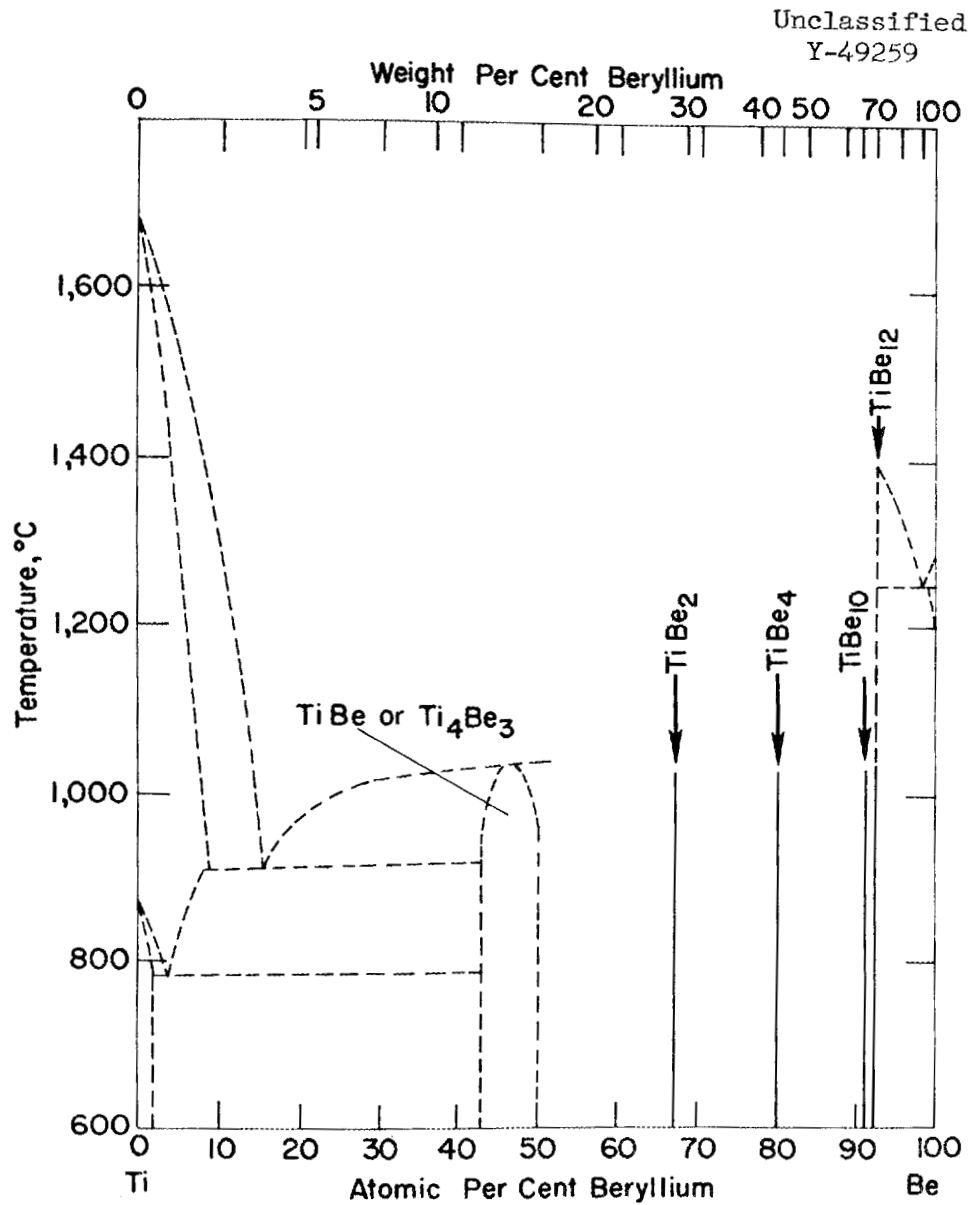


Figure 32. The titanium-beryllium equilibrium diagram.
(Darwin, G. E., and J. H. Buddary, "Alloys and Compounds," Metallurgy of the Rarer Metals - 7 - Beryllium, Academic Press, New York, 1960, pp. 265-320.)

definite identification could be made of the phases present in the microstructure in question.

To summarize, the metallographic examination of each wetting system subjected to the testing condition outlined in Chapter V revealed that only aluminum, zirconium-5 weight per cent beryllium, and titanium-6 weight per cent beryllium caused little or no base-metal reaction with beryllium. Consequently, calculations of the surface energies were performed only for these materials. A discussion of the results of these analyses is presented in the next section.

III. RESULTS OF SURFACE TENSION CALCULATION

Surface energy calculations were performed on systems of beryllium with aluminum, zirconium-5 weight per cent beryllium, and titanium-6 weight per cent beryllium; these systems were found to exhibit minimum reaction at the respective test conditions. The procedures and methods of surface tension calculations are outlined and discussed in the Appendix. The results of these calculations are presented in Table IV.

It must be recognized that these values are the results of calculations of the surface tension properties of liquids saturated with beryllium in contact with that solid phase essentially in equilibrium with the liquid. Although it has been demonstrated that time effects are small, the systems were undergoing slow interface diffusion and surface evaporation due to the dynamic vacuum. The

TABLE IV
RESULTS OF THE SURFACE TENSION DATA CALCULATION

System	Temperature (°C)	Atmos- phere	Contact* Angle (degree)	γ_{LV}^*	γ_{IS}	W_{ad}	S_{IS}
				(dynes per centimeter)			
Aluminum	710	vacuum	142.0	831	2520	176	-1490
Aluminum	760	vacuum	132.0	726	2350	239	-1210
Aluminum	710	argon	116.7	787	2220	434	-1140
Aluminum	760	argon	99.9	561	1960	464	- 658
Zr-5 wt % Be	1030	vacuum	79.8	625	1940	549	- 702
Zr-5 wt % Be	1080	vacuum	64.6	520	1770	614	- 427
Zr-5 wt % Be	1030	argon	97.0	488	1780	576	- 405
Zr-5 wt % Be	1080	argon	79.8	172	1690	569	- 225
Ti-6 wt % Be	1075	vacuum	13.2	492**	1380	970	- 9.00
Ti-6 wt % Be	1125	vacuum	10.8	277	1590	548	- 4.00
Ti-6 wt % Be	1075	argon	8.6	424	1440	844	- 1.00
Ti-6 wt % Be	1125	argon	5.6	329**	1530	660	+ 3.00

*Average of two tests.

**One test only.

inherent inaccuracies associated with impurities in the materials, their assumed final compositions, and the experimental measurements limit the use of the data for other than comparative purposes.

The calculation of the liquid-vapor surface tensions and the resulting calculation of the respective liquid-solid surface tensions were, in general, consistent with the measured contact angles for each of the three systems. Also variations of surface tensions within each system were generally in agreement with variations in contact angles. When the test atmosphere was observed to affect the contact angle, there was a consistent effect on the calculated surface tensions.

A method of analysis employed by Parikh and Humenik (24) is usefully applied to the data presented here. The balance of forces acting at a point of contact between the solid and liquid phases of Figure 1, page 6, is expressed by one form of the Young and Dupré equation (equation 10, page 7),

$$\gamma_{SL} = \gamma_{SV} - \gamma_{LV} \cos \theta \quad .$$

The possible relationships that can occur as a result of these forces are shown graphically in Figure 33 where the liquid-solid surface tension, γ_{LS} , is plotted as a function of the contact angle, θ , for different values of the liquid-vapor surface tension, γ_{LV} . In this graph and for the calculations of surface tension properties presented here, the solid-vapor surface tension, γ_{SV} , is assumed to be equal to 1863 dynes per centimeter.

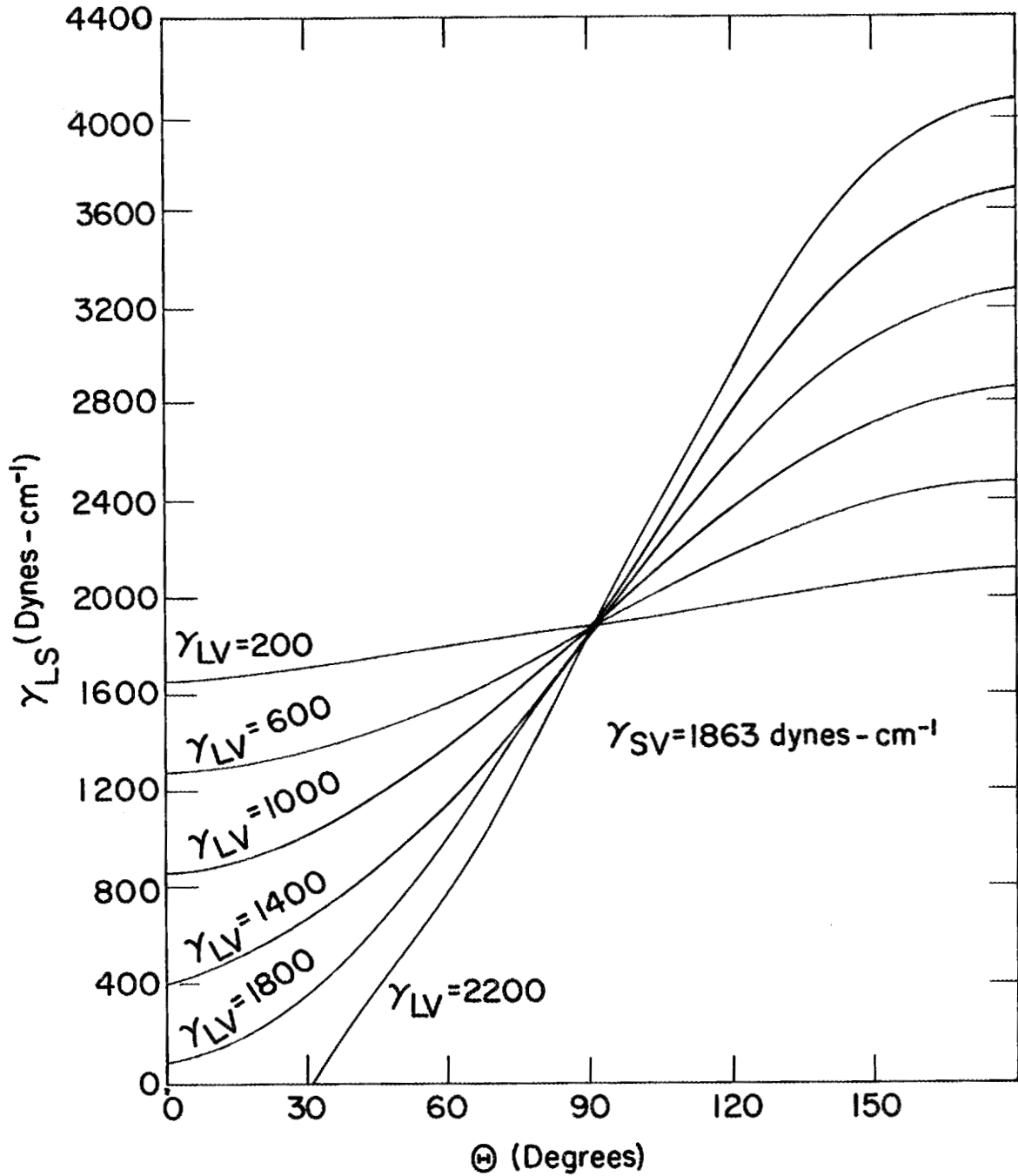
Unclassified
Y-49369

Figure 33. Plot of γ_{LS} versus θ for different values of γ_{LV} . For this study, γ_{SV} is assumed to be 1863 dynes per centimeter.

This general illustration helps to recognize several points related to wettability:

1. When θ equals 90 degrees, γ_{SV} equals γ_{IS} for any value of γ_{LV} .
2. If spreading is taken to be that condition where the contact angle is equal to or is approaching zero, then spreading will occur if γ_{SV} is equal to or greater than γ_{LV} .
3. If θ is less than 90 degrees and γ_{IS} is constant, θ decreases with a decrease in γ_{LV} ; also, if θ is greater than 90 degrees and γ_{IS} is constant, θ increases with a decrease in γ_{LV} .

This type of analysis is valuable; if one can measure γ_{LV} independently, then a prediction can be made as to the possibility of spreading.

For the data presented here, it can be seen that these general relationships have been observed. For observed contact angles near 90 degrees, the calculated γ_{IS} is near the assumed value (1863 dynes per centimeter) of γ_{SV} (see Table IV, page 63). For these systems it is observed that the curve in Figure 33, page 65, is becoming flatter, meaning that the tendency for spreading to occur is increasing.

In the case of the titanium-6 weight per cent beryllium system, the liquid-solid surface tension increases when the testing temperature is raised. The predicted inverse relationship between the change in liquid-solid surface tension versus the change in temperature was observed in the case of the systems of aluminum and zirconium-5 weight per cent beryllium. This discrepancy is probably caused by the

sessile-drop measurement error, which would result in cases of bubbles having very low contact angles or effects resulting from changes in liquid composition.

The work of adhesion, defined as the work required at constant temperature and pressure to pull the interface apart to give clean surfaces, was observed to vary directly with liquid wettability. This variation was typified by the low values of work of adhesion calculated for the nonwetting aluminum system and the high work of adhesion values determined for the wetting system of titanium-6 weight per cent beryllium and zirconium-5 weight per cent beryllium.

The calculated spreading coefficients were negative for all system test conditions included in the study, except in the case of titanium-6 weight per cent beryllium. Negative spreading coefficients indicated a very definite trend. The greater the system wettability, as indicated by lower contact angles and liquid-vapor surface tensions, the greater the numerical magnitude of the spreading coefficient.

Of the three systems used in the calculations, the titanium-6 weight per cent beryllium was observed to provide the greatest wettability on beryllium; the zirconium-5 weight per cent beryllium was next in order. While no basic significance can be given to the absolute values of the surface tension properties calculated, they are useful in indicating the relative tendencies for these liquids to wet beryllium.

CHAPTER VII

CONCLUSIONS AND RECOMMENDATIONS

Conclusions

1. By measurement of contact angles, beryllium wettability by the liquid metals of aluminum, germanium, silver, palladium-2.1 weight per cent beryllium, and titanium-6 weight per cent beryllium is increased when wetting is performed in an argon atmosphere rather than in vacuum. Beryllium wettability by the liquid metals of gold, copper, and zirconium-5 weight per cent beryllium was found to either be unaffected by the testing atmosphere or favor the vacuum over the argon atmosphere.

2. It was established that the wetting behavior of beryllium by liquid metals studied is in agreement with basic wettability theory in that beryllium wetting is promoted by increasing temperature.

3. The results of an extensive metallographic examination of wetting samples tested at all conditions are presented. These data showed that only aluminum, zirconium-5 weight per cent beryllium, and titanium-6 weight per cent beryllium produced little or no alloying with the beryllium. Beryllium alloying of the other liquid metals included in the investigation was so extreme that in some cases liquid phase penetration of greater than 50 per cent of the thickness of the beryllium pad was found.

4. Calculated surface tension properties of those alloy systems found to produce little or no beryllium reaction are presented. These calculations provided a means of relative comparison of the beryllium wetting behavior by these three liquid metals. These data revealed that the liquid-vapor and liquid-solid surface tensions were greater in magnitude for the nonwetting aluminum than for the wetting liquids of titanium-6 weight per cent beryllium and zirconium-5 weight per cent beryllium. Of the three liquid metals submitted for surface tension calculations, titanium-6 weight per cent beryllium was found to have the lowest calculated liquid-vapor and liquid-solid surface tensions; zirconium-5 weight per cent beryllium and aluminum were next in order.

5. Calculations are presented for the work of adhesion and the coefficient of spreading for aluminum, zirconium-5 weight per cent beryllium, and titanium-6 weight per cent beryllium. These data qualitatively indicated that these parameters were greatest for the highly wetting titanium-6 weight per cent beryllium liquid.

Recommendations

1. It is recommended that an investigation be performed to reduce the magnitude of the beryllium solution by more nearly pre-saturating with beryllium the materials of gold, silver, copper, germanium, and the palladium-2.1 weight per cent beryllium binary alloy. Wettability studies similar to those conducted here should then be performed.

2. It is recommended that the effect of beryllium surface preparations on wettability be investigated. While this study did not attempt to determine this effect or the part surface films played on beryllium wettability, it is well known that surface preparation has a marked effect on surface tension properties and that the beryllium oxide film must always be taken into account when considering beryllium surfaces.

APPENDIX

APPENDIX

I. EQUIPMENT

Furnace and Vacuum Equipment

A photograph of the furnace and vacuum system used for the beryllium wetting studies is shown in Figure 34. The furnace consists of a Nichrome wound, resistance heating element capable of attaining a temperature of 1200°C. The furnace is positioned on tracks secured to the workbench to permit it to be readily rolled over the 2-inch-diameter quartz muffle. A tapered glass joint with an optically flat plate on one end was inserted into the tapered joint on the quartz muffle to provide a means of introducing the test specimens and to allow undistorted visual observation of the specimen. The furnace is controlled ($\pm 5^\circ\text{C}$) by an on-off controller, and the sample temperature is continuously monitored by a recorder and a platinum versus platinum-10 per cent rhodium thermocouple positioned in the interior of the muffle immediately adjacent to the sample.

The furnace is equipped with a vacuum system capable of obtaining pressures of less than 10^{-5} torr and an arrangement for introducing an inert gas. High-purity argon, with a nominal analysis as shown in Table V, was further purified by passing it through columbium chips heated to 816°C just before it entered the furnace muffle.

Unclassified
ORNL-Photo-58638

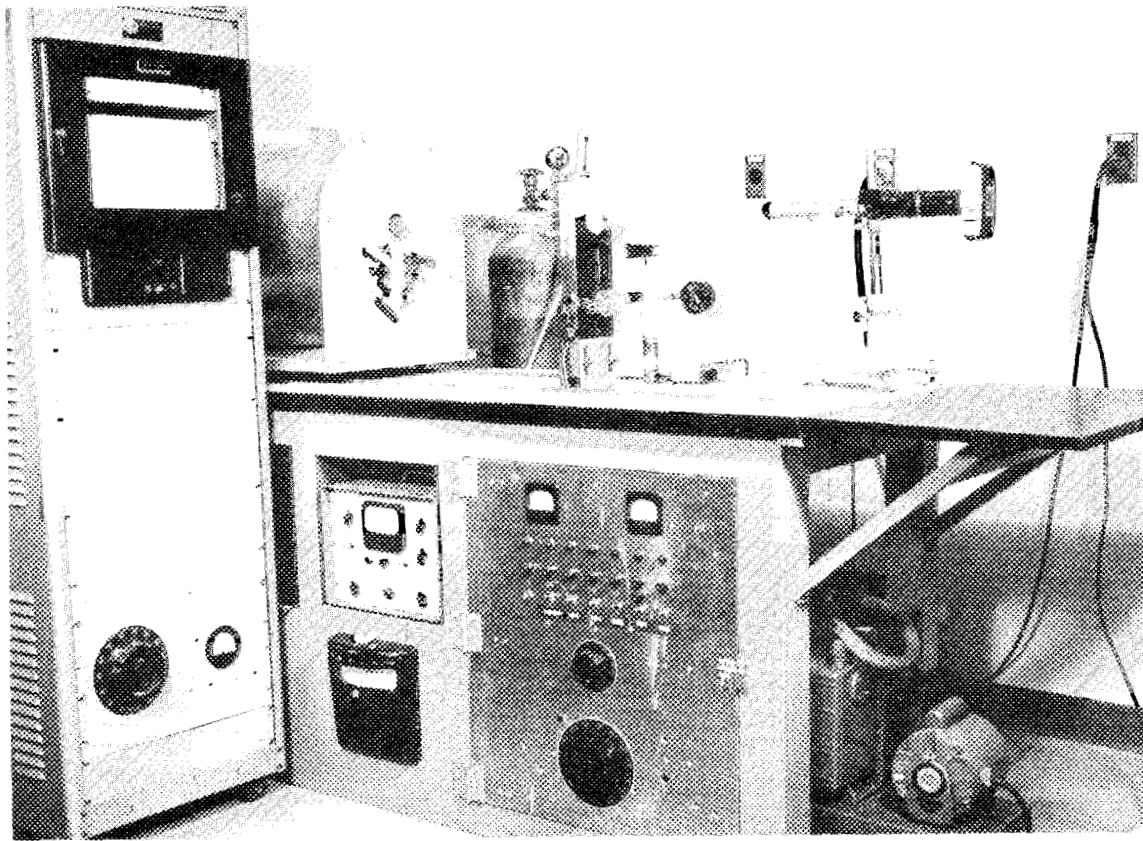


Figure 34. Photograph of furnace and vacuum system used in beryllium wetting study.

TABLE V
NOMINAL CHEMICAL ANALYSIS OF HIGH-PURITY
ARGON USED IN THE WETTING STUDIES

Element	Analysis (vol %)
Oxygen	0.0001
Nitrogen and carbon monoxide	0.0034
Carbon dioxide	0.0002
Hydrogen	0.0003
Argon	99.996

Photographic Equipment

The arrangement for photographing the sessile drops is shown in Figure 35. The drops were viewed through the telemicroscope attached to a Gaertner cathetometer and were photographed with a Baush and Lomb eyepiece camera as shown. Kodak "plus-X" film was used for all photographs.

Arc-Melting Equipment and Procedure

Where necessary, experimental materials used in the wetting experiments were prepared by arc melting using the furnace shown in Figure 36. The furnace chamber was initially pumped to less than 2×10^{-5} torr and was subsequently backfilled with high-purity argon to 2 to 3 pounds per square inch, gage pressure. After gettering the chamber atmosphere by arc melting a zirconium button, the pure metals or alloys were melted five times to ensure good homogeneity. The buttons were then machined into small cubes or were broken up and remelted using the above procedure to obtain pellets of a reduced size.

Metallographic Equipment and Procedure

The test specimens were prepared for metallographic examination by first mounting in clear epoxy resin and sectioning so as to permit observation of the sessile drop-beryllium interface. The mounted and sectioned specimens were then ground flat using a silicon carbide abrasive (approximately 600 grit) dispersed in water. The initial polishing was performed with a nylon cloth-covered vibratory polisher, using 0.3-micron aluminum oxide. The final polishing was performed

Unclassified
Y-48030

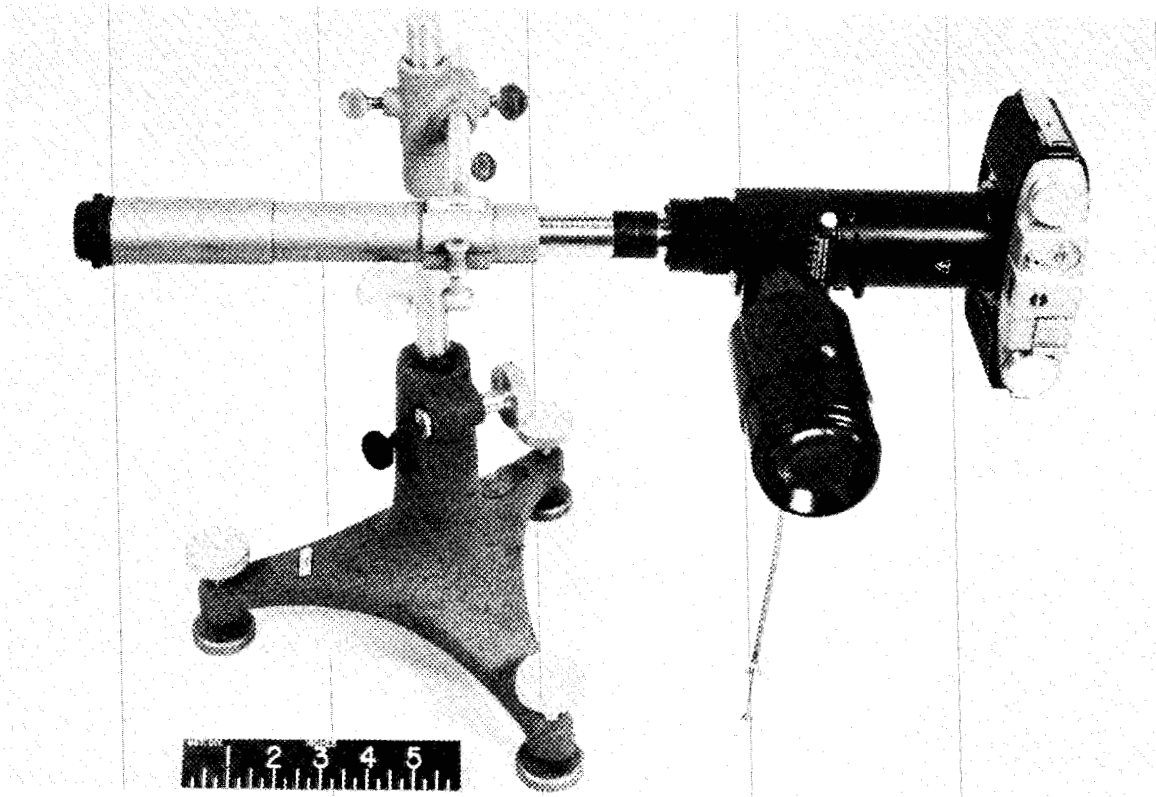


Figure 35. Equipment used in photographing the samples.

Unclassified
Y-21832

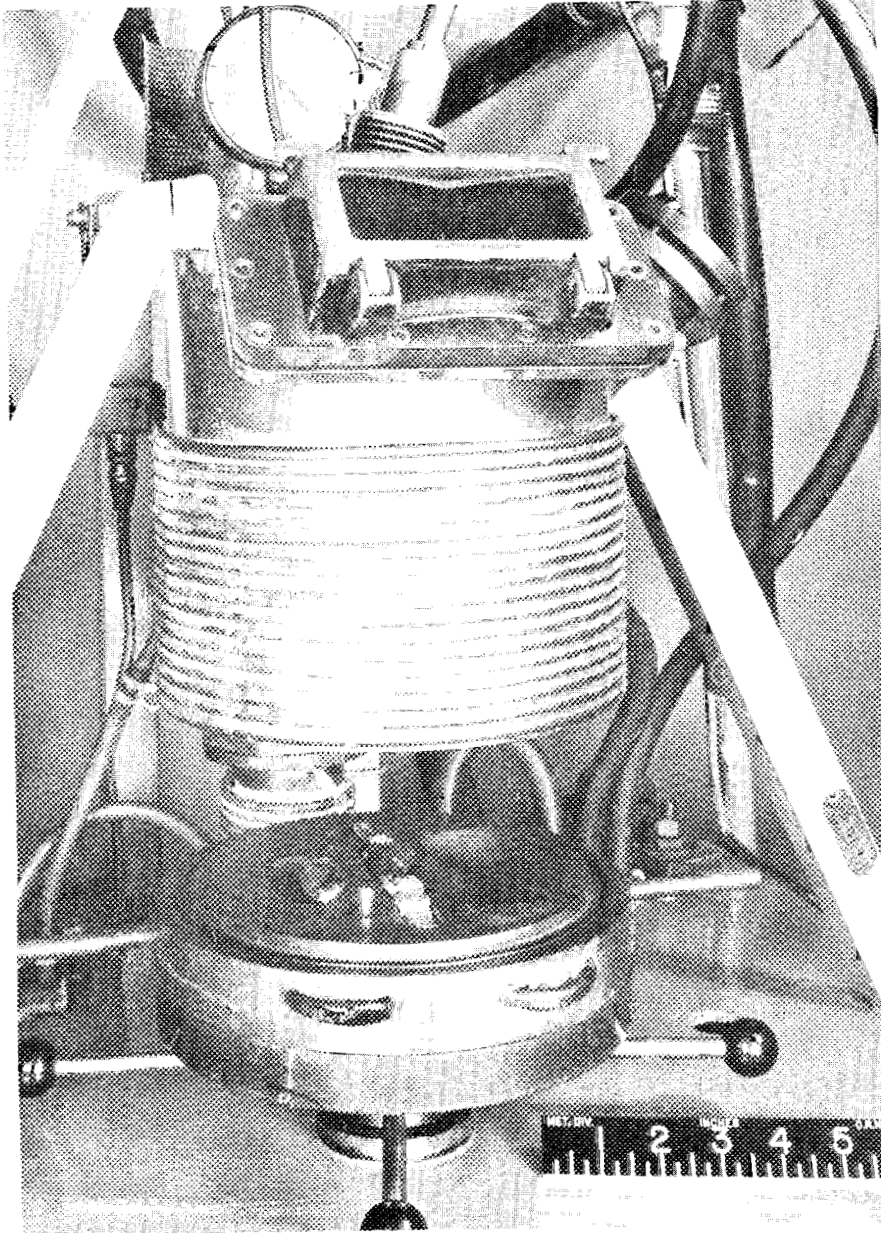


Figure 36. Arc-melting furnace used in preparation of metal buttons.

with another vibratory polishing machine covered with a deep-nap cloth with 0.1-micron aluminum oxide-ethylene glycol slurry as the abrasive. The specimens were then washed in hot water, rinsed with absolute ethyl alcohol, and dried in an air blast.

The specimens were examined and photographed using either polarized or bright-field illumination. No etchant was needed on the samples wetted with the binary alloys of titanium-6 weight per cent beryllium and zirconium-5 weight per cent beryllium. The etchants used on the samples wetted with the pure metals and the palladium-2.1 weight per cent beryllium binary alloy were:

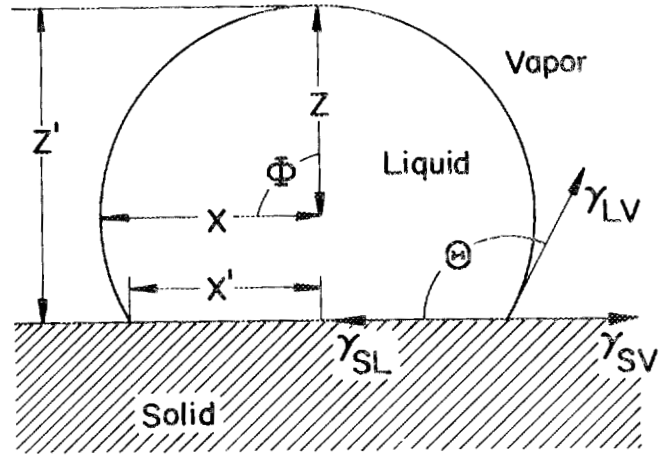
Aluminum	-	HNO ₃ , HCl, HF, H ₂ O
Silver	-	No etchant required
Copper	-	C ₂ H ₅ OH, HCl, FeCl ₃
Gold	-	Aqua regia
Germanium	-	HNO ₃ , HF, HC ₂ H ₃ O ₂
Palladium-2.1 wt % beryllium-		KCN, (NH ₄) ₂ S ₂ O ₃ or aqua regia

II. SAMPLE CALCULATIONS

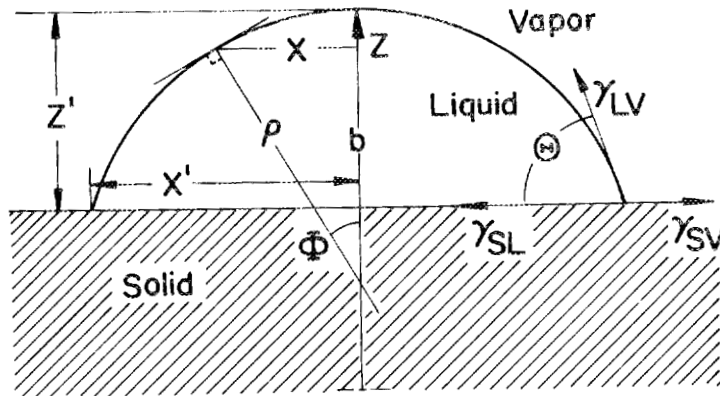
The Sessile-Drop Method

The determination of the surface tension by means of the sessile-drop method depends on the attainment of equilibrium between forces of surface tension and of gravity. When this premise is satisfied, a molten metal drop rests on a solid surface as illustrated in Figure 37.

Unclassified
Y-49252



A. FOR $\theta > 90^\circ$



B. FOR $\theta < 90^\circ$

Figure 37. Sessile drops at rest for the cases where θ is greater than 90 degrees and θ is less than 90 degrees.

The fundamental equation of surface tension at any point requires

$$\gamma_{LV} \left(\frac{1}{R} + \frac{1}{R'} \right) = P = gdz + c \quad (12)$$

where

γ_{LV} = liquid-vapor surface tension,

R = principal radius of curvature for surface perpendicular to the plane of Figure 37, * page 79,

R' = principal radius of curvature for surface in the plane of Figure 37, * page 79,

P = pressure,

c = constant,

g = gravitational acceleration

d = density

Z = axis of rotation,

z = distance along Z -axis.

*The two radii of curvature (R, R') for some arbitrarily curved surface are obtained by erecting a normal to the surface at any point on the surface and then passing a plane through the surface which contains the normal. The line of intersection will in general be curved. The radius of curvature is that radius for a circle tangent to the curved line at the point in question. The second radius of curvature is obtained by passing a second plane through the surface also containing the normal, but perpendicular to the first plane. This gives a second curved line of intersection and a second radius of curvature.

If ρ is taken as the radius of curvature of a meridional section and ϕ is the angle between ρ and z then $R = \rho$ and $R' = x/\sin \phi$.

Equation 12 then reduces to

$$\gamma_{LV} \left(\frac{1}{\rho} + \frac{\sin \phi}{x} \right) = g dz + c \quad (13)$$

If b is defined as the radius of curvature at the drop apex, then at the apex $\rho = b$, $x/\sin \phi \rightarrow b$, and $z = 0$. Therefore, from equation 13

$$c = \frac{2 \gamma_{LV}}{b} \quad (14)$$

By substitution and multiplying by b , equation 12 becomes

$$\frac{1}{(\rho/b)} + \frac{\sin \phi}{(x/b)} = 2 + \frac{gd b^2}{\gamma_{LV}} \left(\frac{z}{b} \right) \quad (15)$$

If the quantity $\frac{gd b^2}{\gamma_{LV}}$ is defined as β , we have

$$\frac{1}{(\rho/b)} + \frac{\sin \phi}{(x/b)} = 2 + \beta \frac{z}{b} \quad (16)$$

By developing differential increments of this relationship, Bashforth and Adams (21) prepared tables of β and x/z for $\phi = 90$ degrees and x/b for various values of β and ϕ . The measurement of x and z shown in Figure 37 makes it possible to determine β and b from the tables and the surface tension is then calculated from the relation

$$\gamma_{LV} = \frac{gd b^2}{\beta} \quad (17)$$

Using x , x' , z' , θ , b , and β the drop volume can be calculated from the relationships of the following situations:
for cases where θ is greater than 90 degrees

$$V = \frac{\pi b^2 (x')^2}{b} \left[\frac{2}{b} - \frac{2 \sin \theta}{x} + \frac{\beta z'}{b^2} \right] \quad (14) \quad (18)$$

for cases where θ is less than 90 degrees

$$V = \frac{\pi}{6} [(z')^3 + 3(z')(x')^2] \quad (14) \quad (19)$$

Typical Calculation of γ_{LV}

For θ greater than 90 degrees. To obtain $\frac{g b^2}{\beta}$: The test sample used for the calculation of a typical liquid-vapor surface tension, γ_{LV} , is that of aluminum wetted on beryllium in vacuum at 760°C (Figure 9, page 25), which has a contact angle, θ , measured to be 127.0 degrees. The measurements on the aluminum drop were taken from the photograph exposed after 150 seconds at that temperature. Referring to Figure 37(a), page 79, the parameters were found to be

$$\begin{aligned} x &= 0.259 \text{ centimeter} \\ z &= 0.246 \text{ centimeter} \\ x' &= 0.172 \text{ centimeter} \\ z' &= 0.446 \text{ centimeter} \\ x/z &= 1.050, \text{ when } \phi = 90 \text{ degrees.} \end{aligned}$$

Referring to the portion of the Bashforth and Adams tables relating values of β to $(\frac{x}{z})_{\phi = 90^\circ}$ and interpolating, the following is obtained:

$$\beta = \frac{g d b^2}{\gamma_{LV}} = 0.25 \quad .$$

Referring next to the portion of the tables giving values of x/b and z/b in terms of β and ϕ , linear interpolation provides $\phi = 90$ degrees, $\beta = 0.25$, $x/b = 0.96312$, and $z/b = 0.91699$. Knowing

both x and z by direct measurement, b is calculated to be 0.268 centimeter. By combining this with previous data, the following equation is obtained:

$$\gamma_{IV} = \frac{gd b^2}{\beta} = 282.0 \text{ d} .$$

To obtain density: From the values of x , x' , z' , b , and β measured or determined above, the volume was calculated using equation 18 to be 0.0665 cubic centimeter. The weight of the aluminum was 0.1644 gram. Using these values of drop volume and weight, the density equals $\frac{0.1644}{0.0665}$ equals 2.47 grams per cubic centimeter.

To obtain surface tension: By combining the results of the calculations obtained for $\frac{g b^2}{\beta}$ and density above, it is found that for the aluminum molten drop on beryllium at 760°C in vacuum the liquid surface tension is

$$\gamma_{IV} = \frac{gd b^2}{\beta} = 697 \text{ dynes per centimeter.}$$

For θ less than 90 degrees. To obtain $\frac{g b^2}{\beta}$: The sample used for a typical surface tension calculation for the case where θ is less than 90 degrees is the zirconium-5 weight per cent beryllium binary alloy in vacuum at 1030°C. The molten alloy drop is shown in Figure 10, page 26. The contact angle, θ , was measured to be 77.1 degrees.

The measurements were taken on the molten drop after 150 seconds at test temperature. The radius of curvature of the drop at its apex, b , was geometrically found to be 0.273 centimeter. Referring to Figure 37(b), page 79, the measurement of the following parameters yielded:

$$z' = 0.195 \text{ centimeter}$$

$$x' = 0.251 \text{ centimeter}$$

at $\phi = 60$ degrees

$$x = 0.220 \text{ centimeter}$$

$$z = 0.114 \text{ centimeter}$$

$$x/b = 0.806$$

$$z/b = 0.418.$$

Referring to the Bashforth and Adams tables giving values of x/b and z/b in terms of β and ϕ , we obtain by linear interpolation $\phi = 60$ degrees, $x/b = 0.806$, $z/b = 0.418$, and $\beta = 0.968$. Combining these measured or calculated parameters, the following equation is obtained:

$$\gamma_{LV} = \frac{gd b^2}{\beta} = 75.3 \text{ d} .$$

To obtain density: From the values of x' and z' obtained by measurement of the photograph of the molten drop photograph, the volume was calculated, using equation 19, page 82, to be 0.0232 cubic centimeter. The weight of the zirconium-5 weight per cent beryllium alloy drop was 0.1457 gram. The values of drop volume and weight gave a calculated density of 6.28 grams per cubic centimeter.

To obtain surface tension: Using the values calculated for $\frac{gd b^2}{\beta}$ and density above, the liquid-vapor surface tension of the zirconium-5 weight per cent beryllium alloy at 1030°C in vacuum on beryllium was found to be

$$\gamma_{LV} = \frac{gd b^2}{\beta} = 473 \text{ dynes per centimeter} .$$

Typical Calculation of γ_{SL} , W_{ad} , and S_{LS}

The interfacial liquid-solid surface tension, γ_{SL} , can now be calculated using equation 10, page 7. The solid-vapor surface tension, γ_{LV} , of beryllium was assumed to be constant over the temperature range studied and equal to 1863 dynes per centimeter (25). A typical calculation using the aluminum system for θ greater than 90 degrees (page 82) is presented below.

Liquid-solid surface tension, γ_{SL} :

$$\gamma_{SL} = \gamma_{SV} - \gamma_{LV} \cos \theta = 1863 - (697) \cos 127^\circ$$

$$\gamma_{SL} = 2280 \text{ dynes per centimeter .}$$

The calculation of the liquid-solid spreading coefficient, S_{LS} , and the work of adhesion can next be calculated using equations 6 and 11, pages 5 and 7, respectively. Typical calculations for these parameters for the case of the high-temperature, vacuum-atmosphere aluminum system are presented below.

Spreading coefficient, S_{LS} :

$$S_{LS} = \gamma_{SV} - (\gamma_{LV} + \gamma_{LS}) = 1863 - (697 + 2280)$$

$$S_{LS} = -1110 \text{ dynes per centimeter .}$$

Work of adhesion, W_{ad} :

$$W_{ad} = (\gamma_{LV}) (1 + \cos \theta) = (697) (1 + \cos 127.0^\circ)$$

$$W_{ad} = 267 \text{ dynes per centimeter .}$$

The methods and procedures presented above for the calculation of surface tension data were used throughout the study.

LIST OF REFERENCES

LIST OF REFERENCES

1. Pahler, Robert E., "The Role of Beryllium in the Atomic Energy Program," The Metal Beryllium, American Society for Metals, Cleveland, Ohio, 1955, pp. 14-23.
2. Darwin, G. E., and J. H. Buddary, "Occurrence, Work Pressures, and Uses of Beryllium," Metallurgy of the Rarer Metals - 7 - Beryllium, Academic Press, New York, 1960, pp. 1-10.
3. Beaver, W. W., and D. W. Lillie, "Beryllium Metal, Alloys and Compounds," Reactor Handbook, Vol. 1, Materials, Interscience Publishers, New York, 1960, pp. 897-942.
4. Coobs, J. H., "Advanced Materials Development," Information Meeting on Gas-Cooled Power Reactor, Oak Ridge National Laboratory, October 21-22, 1958, USAEC Report, TLD-7564 (December, 1958), pp. 363-372.
5. Eaton, N. F., J. Skinner, and A. J. Martin, Welding and Metal Fabrication, 28(2), 46-52 (1960).
6. Martin, D. C., "Joining of Beryllium," The Metal Beryllium, American Society for Metals, Cleveland, Ohio, 1955, pp. 283-294.
7. Hawkins, W. D., Physical Chemistry of Surfaces, Reinhold Publishing Corporation, Inc., New York, 1952.
8. Bondi, A., "Spreading of Liquid Metals on Solid Surfaces; Surface Chemistry of High-Energy Substances," Chem. Rev., 52(2), 417-458 (1953).
9. Cohen, J. B., Beryllium Joining RAD Sponsored Program, Wright Air Development Corporation Report, WADC-TR-59-695, Part 1 (1960).
10. Monroe, R. E., D. C. Martin, and C. B. Voldrich, Welding and Brazing of Beryllium to Itself and to Other Metals, USAEC Report, BMI-836 (May 28, 1953).
11. Zunick, M. J., and J. E. Illingworth, Mater. & Methods, 39(3), 95 (1954).
12. Wikle, K. G., and R. Magalski, Brazing Beryllium Tubing to High-Temperature Alloy Collars, USAEC Report, COO-310 (June, 1956).
13. Gilliland, R. G., and G. M. Slaughter, "Fusion Welding of End Caps in Beryllium Tubes," Welding J., 42(1), 29-36 (January, 1963).

14. Ellefson, B. S., and N. W. Taylor, "Surface Properties of Fused Salts and Glasses: Parts I and II," J. Am. Ceram. Soc., 21(6), 193-213 (1938).
15. Weare, N. E., and R. E. Monroe, Joining of Beryllium, Defense Metals Information Center Memorandum 13, Battelle Memorial Institute (March 30, 1959).
16. Oak Ridge National Laboratory, Gas-Cooled Reactor Quarterly Progress Report for Period Ending December 31, 1959, ORNL-2888, pp. 94-97.
17. Oak Ridge National Laboratory, Gas-Cooled Reactor Quarterly Progress Report for Period Ending March 31, 1960, ORNL-2929, pp. 140-142.
18. Oak Ridge National Laboratory, Gas-Cooled Reactor Quarterly Progress Report for Period Ending June 30, 1960, ORNL-2964, pp. 138-141.
19. Quincke, G., Ann. Phys. Chem., 135, 621 (1868); 138, 141 (1869).
20. Adam, N. K., Physics and Chemistry of Surfaces, Oxford University Press, New York, 1930, pp. 12-14.
21. Bashforth, F., and J. C. Adams, An Attempt to Test Theories of Capillarity, Cambridge University Press, England, 1883.
22. Hansen, M., Constitution of Binary Alloys, McGraw-Hill, New York, 1958.
23. Darwin, G. E., and J. H. Buddary, "Alloys and Compounds," Metallurgy of the Rarer Metals - 7 - Beryllium, Academic Press, New York, 1960, pp. 265-320.
24. Parikh, N. M., and M. Humenik, Jr., "Cermets: II, Wettability and Microstructure Studies in Liquid-Phase Sintering," J. Am. Ceram. Soc., 40(9), 315-320 (1957).
25. Taylor, J. W., "Wetting by Liquid Metals," Progr. Nucl. Energy Ser. V, 2, 398-416 (1959).

BIBLIOGRAPHY

BIBLIOGRAPHY

- Adamson, A. W. Physical Chemistry of Surfaces. New York: Interscience Publishers, 1960. 629 pp.
- Allen, B. C., and W. D. Kingery. "Surface Tension and Contact Angles in Some Liquid Metal-Solid Ceramic Systems," Transactions of the Metallurgical Society of AIME, 215:30-37, 1959.
- Bailey, G. L. J., and H. C. Watkins. "The Flow of Liquid Metals on Solid Metal Surfaces and Its Relationship to Soldering, Brazing, and Hot-Dip Coating," Journal of the Institute of Metals, 80[2]:57-76, 1951.
- Bikerman, J. J. Surface Chemistry for Industrial Research. New York: Academic Press, 1948. 464 pp.
- Burdon, R. S. Surface Tension and the Spreading of Liquids. Second edition. England: Cambridge University Press, 1949. 92 pp.
- Gregg, S. J. Surface Chemistry of Solids. New York: Reinhold Publishing Corporation, Incorporated, 1951. 393 pp.
- Kingery, W. D. "Role of Surface Energies and Wetting in Metal-Ceramic Sealing," American Ceramic Society Bulletin, 35[3]:108-112, 1956.
- Kingery, W. D., and M. Humenik, Jr. "Surface Tension at Elevated Temperatures. I. Furnace and Method for Use of the Sessile Drop Method; Surface Tension of Silicon, Iron, and Nickel," Journal of Physical Chemistry, 57:359-363, 1953.
- Milner, D. R. "A Survey of the Scientific Principles Related to Wetting and Spreading," British Welding Journal, 5:90-105, 1958.
- Smith, C. S. Grains, Phases, and Interfaces: An Interpretation of Microstructure, American Institute of Mining and Metallurgical Engineers Technical Publication No. 2387, June, 1948.
- Wall, A. J., and D. R. Milner. "Wetting and Spreading Phenomena in a Vacuum," Journal of the Institute of Metals, 90[10]:394-402, 1962.
- Williams, J. C., and J. W. Neilson. "Wetting of Original and Metallized High-Alumina Surfaces by Molten Brazing Solders," Journal of the American Ceramic Society, 42:229-235, 1959.

ORNL-3438
UC-25 - Metals, Ceramics, and Materials
TID-4500 (20th ed.)

Internal Distribution

1-2.	Central Research Library	59.	E. Hoffman
3.	Reactor Division Library	60.	J. T. Howe
4-5.	ORNL - Y-12 Technical Library, Document Reference Section	61.	P. J. Kreyger
6-25.	Laboratory Records Department	62.	C. E. Larson
26.	Laboratory Records, ORNL-RC	63.	C. F. Leitten
27.	ORNL Patent Office	64.	H. G. MacPherson
28.	Russell Baldock	65.	W. D. Manly
29.	J. O. Betterton, Jr.	66.	W. R. Martin
30.	W. H. Bridges	67.	H. E. McCoy
31.	R. E. Clausing	68.	E. C. Miller
32.	J. E. Eorgan	69.	R. L. Shipp, Jr.
33.	C. W. Fox	70.	G. M. Slaughter
34.	J. H. Frye, Jr.	71.	J. A. Swartout
35-49.	R. G. Gilliland	72.	J. W. Tackett
50.	A. Goldman	73.	W. C. Thurber
51.	R. J. Gray	74.	A. M. Weinberg
52.	J. P. Hammond	75.	A. A. Burr (consultant)
53.	R. L. Heestand	76.	J. R. Johnson (consultant)
54-58.	M. R. Hill	77.	C. S. Smith (consultant)
		78.	R. Smoluchowski (consultant)

External Distribution

79-80.	David F. Cope, ORO
81.	D. E. Baker, GE Hanford
82.	Ersel Evans, GE Hanford
83.	J. L. Gregg, Cornell University
84.	J. Simmons, AEC, Washington
85.	E. E. Stansbury, University of Tennessee
86.	Donald K. Stevens, AEC, Washington
87.	Nathaniel Stetson, SRO
88-591.	Given distribution as shown in TID-4500 (20th ed.) under Metals, Ceramics, and Materials category